Journal of Environmental Chemical Engineering 6 (2018) 3531–3555

Contents lists available at ScienceDirect

Journal of Environmental Chemical Engineering

journal homepage: www.elsevier.com/locate/jece

Recent advances in photocatalysis for environmental applications

Ciara Byrne[a,b], Gokulakrishnan Subramanian[c], Suresh C. Pillai[a,b,*]

[a] Nanotechnology and Bio-Engineering Research Division, Department of Environmental Science, School of Science, Institute of Technology Sligo, Ash Lane, Sligo, Ireland
[b] Centre for Precision Engineering, Materials and Manufacturing Research (PEM), Institute of Technology Sligo, Ash Lane, Sligo, Ireland
[c] Department of Chemistry, Birla Institute of Technology and Science, Pilani, K.K. Birla, Goa Campus, NH17B, Zuarinagar, Goa, 403 726, India

ABSTRACT

Advanced Oxidation technologies (AOTs) are gaining attention as an effective waste water treatment methodology capable of degrading diverse spectrum of recalcitrant organic contaminants and microbes. Undoubtedly, photocatalysis is a promising AOT to alleviate the problem of water pollution. Despite recent research into other photocatalysts (e.g. ZnO, ZnS, Semiconductor-Graphene composites, perovskites, MoS_2, WO_3 and Fe_2O_3), titanium dioxide (TiO_2) remains the most popular photocatalyst due to its low cost, nontoxicity and high oxidising ability. Moreover, titania photocatalysts can easily be immobilized on various surfaces and be scaled up for large scale water treatment. The current review aims to highlight recent advancements in photocatalytic AOTs with main emphasis on TiO_2 photocatalysis. This review also discusses the use of TiO_2 photocatalysis for water and waste treatment, treating contaminants of emerging concern (CECs), pesticides, endocrine disrupters (EDs) and bacteria using both UV and visible light irradiations. It was concluded that with efficient photoreactor configuration and further studies on the photocatalyst regeneration, TiO_2 photocatalysis is a viable option for the reclamation of agricultural/irrigational waste water. Novel doped photocatalysts such as ZnS-CuS-CdS, carbon spheres/CdS, g-C_3N_4-Au-CdS, ZnS-WS_2-CdS, C_3N_4-CdS and Pd-Cr_2O_3-CdS have also been discussed. Finally, the advances in the actively studied metal organic framework based photocatalysts that are emerging as effective alternate for metal oxide based photocatalysts is also discussed in detail.

1. Introduction

Photochemical AOPs are the most preferred because they offer the possibility of utilizing naturally available and renewable solar energy as light source for photochemical waste remediation, thereby making the process green and sustainable. TiO_2 photocatalysis and photo-Fenton are two popular photochemical AOPs. Among them, TiO_2 photocatalysis has gained particular interest because of heterogeneous nature that offers the possibility of catalyst reuse. In addition, it can operate at wide pH range unlike photo-Fenton process. TiO_2 is environmentally benign, biocompatible, abundantly available, highly stable and low cost metal oxide photocatalyst with ability to efficiently degrade a spectrum of contaminants [1–17]. TiO_2 can be immobilized in to a variety of supports without much loss of its photocatalytic efficiency. This important feature favours the development of TiO_2 photocatalytic process for constructing efficient photochemical reactors for air and water purification. Moreover, intense research on TiO_2 to shift its optical response from UV to visible light has produced some interesting visible light active TiO_2 materials that utilize much available visible light of solar radiation for water decontamination [3–15,18–20].

The ability of TiO_2 to act as a photocatalyst was first discovered approximately 90 years ago [19,21]. However, it did not become an extensively researched area until Fujishima and Honda discovered that TiO_2 electrode could be used to photocatalytically split water in 1972 [19,21–24]. In the decades since this discovery, there has been extensive research in understanding the photocatalytic process and attempting to improve the efficiency of using TiO_2 as a photocatalyst [22]. There also has been a significant number of publications examining the applications photocatalysts, *e.g.* water or air decontamination and self-cleaning surfaces [19,25]. The reactions for heterogeneous photocatalysis occur at the surface of the semiconductor material.

Photocatalysis is initiated by the photocatalyst (e.g. semiconductor TiO_2) being bombarded with photons from UV light (from an artificial source or solar light) [18,22]. These photons cause the electrons (e^-) on the surface photocatalyst to become 'excited' in the valance band if the energy of the photons is greater than the band gap, this causes the e^- to go up into the conduction band, see Fig. 1 [1,18,19]. Once the e^-

* Corresponding author at: Nanotechnology and Bio-Engineering Research Division, Department of Environmental Science, School of Science, Institute of Technology Sligo, Ash Lane, Sligo, Ireland.
E-mail address: pillai.surech@itsligo.ie (S.C. Pillai).

http://dx.doi.org/10.1016/j.jece.2017.07.080
Received 15 November 2016; Received in revised form 29 July 2017; Accepted 31 July 2017
Available online 03 August 2017

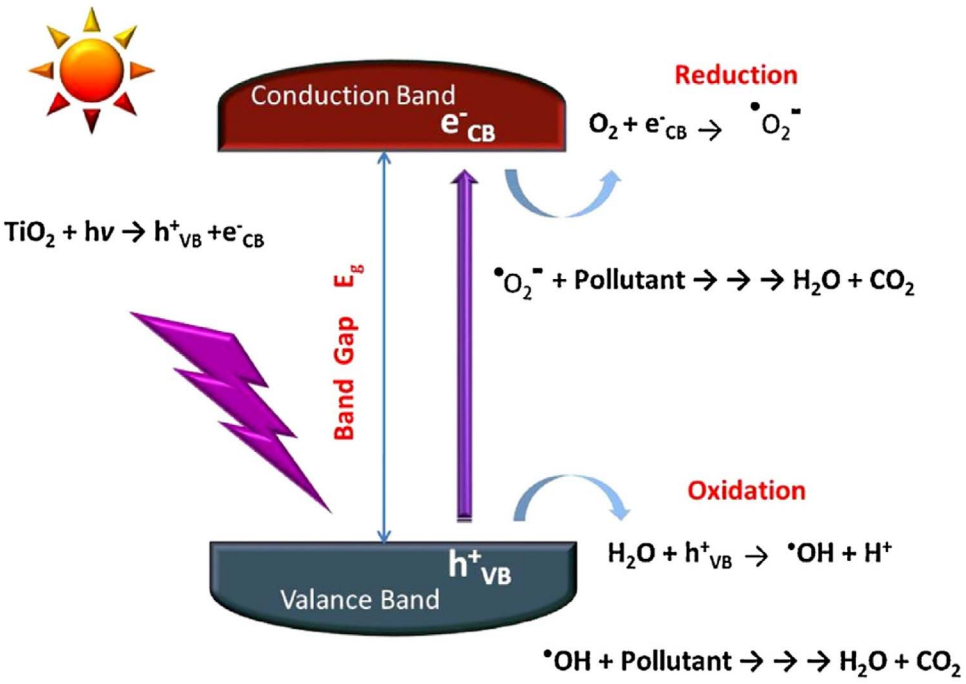

Fig. 1. Mechanism of photocatalysis. (Banerjee et al., *Appl.Catal.BEnviron.*176–177(2015)396). Copyright 2015, reprinted with permission from Elsevier.

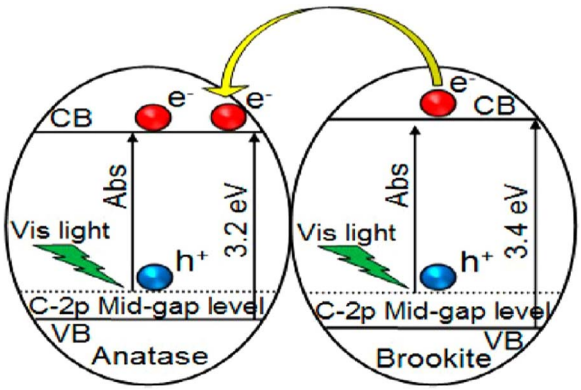

Fig. 2. Heterojunction photocatalysis with anatase and brookite phase [52]. (Etacheri et al., ACS Appl. Mater. Interfaces 1663–1672 (2013) 5). Copyright 2013, reprinted with permission from American Chemical Society.

have absorbed to the conduction band (e^-_{CB}), a positive hole is formed on valence band (h^+_{VB}) (Eq. (1) and Fig. 1) [1,26–28].

$$TiO_2 + h\nu \rightarrow h^+_{VB} + e^-_{CB} \quad (1)$$

The excited electrons that are now in the conduction band (e^-_{CB}) will react with oxygen (O_2), which produces superoxide radicals ($O_2{}^-$), or hydroperoxide radicals (HO_2), see Fig. 1 and Eq. (2) [26,29,30]. These reactive oxygen species are then used for the degradation of pollutants into water (H_2O) and carbon dioxide (CO_2), see Fig. 1 [31,32]. The superoxide radicals can also be used for secondary degradation steps [33]. While this reaction is occurring, the oxidation of water takes place at the positive hole in the valance band (h^+_{VB}) [26]. This reaction generates hydroxyl radicals (OH) and hydrogen ions (H^+), see Fig. 1 and Eq. (3) [26]. The OH reacts with pollutants present and forms H_2O and CO_2.

$$e^-_{CB} + O_2 \rightarrow O_2{}^- \quad (2)$$

$$h^+_{VB} + H_2O \rightarrow OH + H^+ \quad (3)$$

In the last decade or so, the ability to sensitise a photocatalyst that is activated by UV and visible light has gained significant interest [19]. One method that has been examined is using photocatalysts which have smaller band gabs then the band gap of TiO_2, these are discussed in a section below [19].

However, even with an increased interest in developing a new photocatalyst, TiO_2 still remains one of the most researched

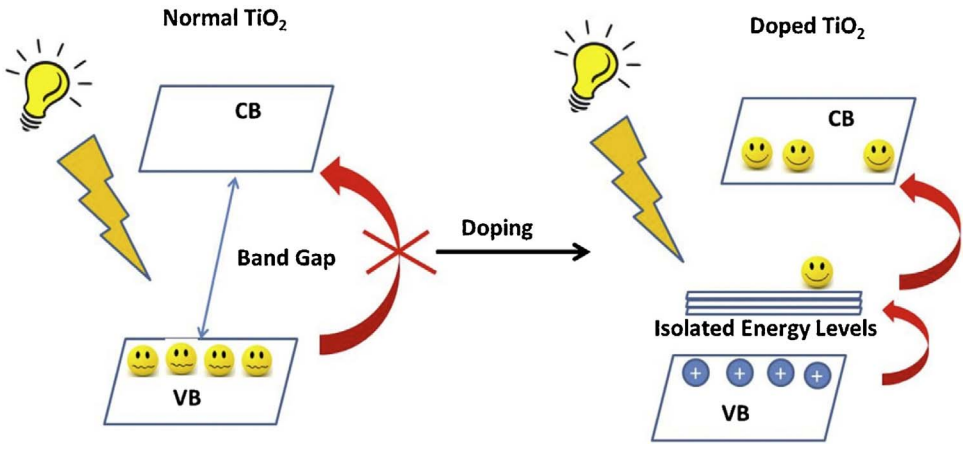

Fig. 3. General principle of narrowing the band gap with a dopant [74]. (Etacheri et al., J. Photochem. & Photobio. C: Photochem. Rev. 1–29 (2015) 25).Copyright 2015, reprinted with permission from Elsevier.

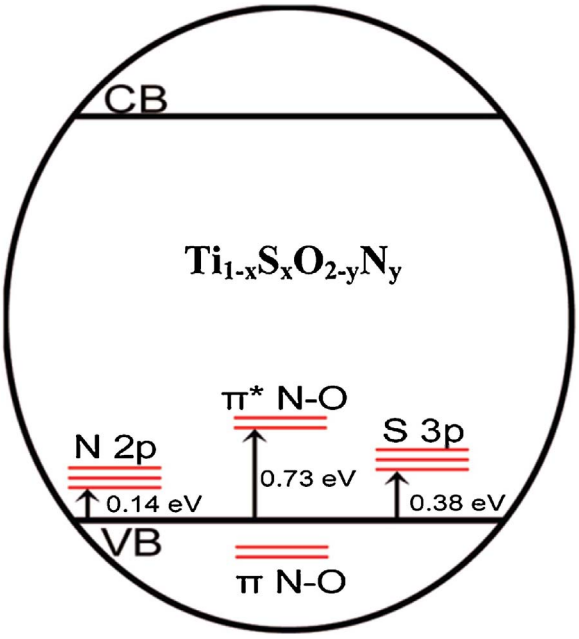

Fig. 4. Electron Structure of Ti$_1$-xSxO2-xNy, showing the presence of impurity energy states [24,26,94]. (Etacheri et al., *ACS Inorg. Chem.* 7164–7173 (2012) 51). Copyright 2012, reprinted with permission from American Chemical Society.

photocatalyst. This is due to its ease of preparation, cost efficacy, nontoxicity, long term stability and strong oxidising ability [18,34–40]. TiO_2 has three main phases, which are anatase, brookite and rutile [1,20,35,36,41–50]. The anatase phase is considered the most photocatalytic active phase due to its large band gap, 3.2 eV [19,35,37,51,52]. However, despite all the benefits of using TiO_2 as a photocatalyst there is one major disadvantage. At present, TiO_2 can only utilise the UV light (< 390 nm) in solar irradiation due to its large band gap (anatase = 3.2 eV). [19] Solar light is made up of only 4% of UV but visible light counts for approximately 42% of solar light [1,53]. A visible light (400–700 nm) active, high temperature (≥1000 °C) stable anatase phase is required for many of its applications [49].

2. Improvements on TiO_2 photocatalytic activity

There a number of ways to improve the rate of photocatalytic activity and producing a TiO_2 photocatalyst that utilises both UV and visible light.

One solution to these problems is the use of a TiO_2 heterojunction photocatalyst. While anatase is commonly considered the most photocatalytically active phase of TiO_2, there have been studies that have reported that the use of two phases (anatase and brookite or anatase and rutile) as a heterojunction can improve the photocatalytic activity when compared with the use of anatase alone, see Fig. 2 [1,54–59]. This improvement is due to the effect it has on the charge carrier separation, as it leads to trapping the electrons in the rutile phase and minimises the electron-hole recombination [60–62]. There have been reports that the electrons are trapped within the lattice while simultaneously the trapping of holes on the surface occurs [18,60,63]. The 'excited' state electrons in the conduction band in brookite can be transferred into the conduction band of anatase [52]. This is due to the conduction band of brookite being approx. 0.2 eV higher than the anatase conduction band [52]. This transfer reduces the rate of electron-hole recombination and improves the visible light photocatalytic activity. [52] This is similar to heterojunctions between two different photocatalysts (Fig. 2).

Numerous studies use the reference material, P-25 (previously manufactured by Degussa but now made by Evonik Industries), which is a mixed phase (anatase and rutile) TiO_2 photocatalyst, for comparison with work being completed [18,19]. It is considered that the enhanced performance of this material is due to its high specific surface area [18,64]. The material is generally comprised of 80 wt% anatase and 20 wt% rutile [18]. A 70 wt% anatase and 30 wt% rutile sample displayed a larger surface area and increased photocatalytic ability when compared with Degussa P-25, with surface areas being 72 m^2/g and 49 m^2/g respectively [59]. However, caution must be taken when comparing the materials photoactivity based on the ratio of each phase as the method of synthesis has a significant impact on particle size and surface area [18]. The precursor used calcination temperature and pH directly affects the parameters such as surface area, morphology, and phase distribution obtained during sol–gel synthesis [56,58,59,65–73]. A mixed phase sample with the desired ratio of wt% can be produced by altering the kinetics of the reaction [18]. However, the effects of each of the following must be comprehended so this can happen: temperature;

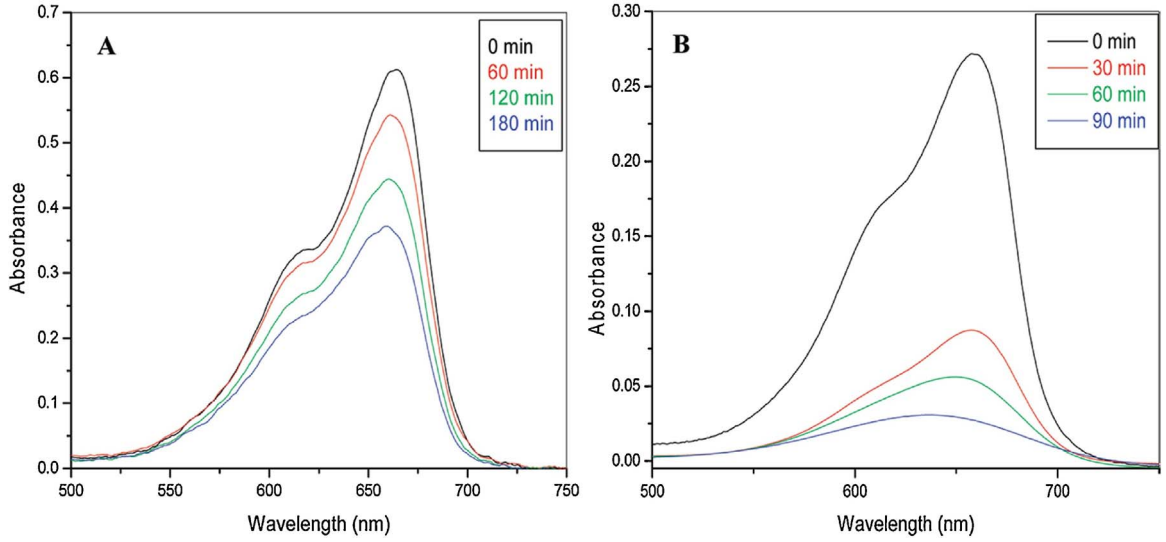

Fig. 5. UV spectra analysis of visible-light induced organic dye degradation using (A) Degussa P-25 and (B) N,S doped TiO_2 sample [95]. (Etacheri et al., *ACS Inorg. Chem.* 7164−7173 (2012) 51). Copyright 2012, reprinted with permission from American Chemical Society.

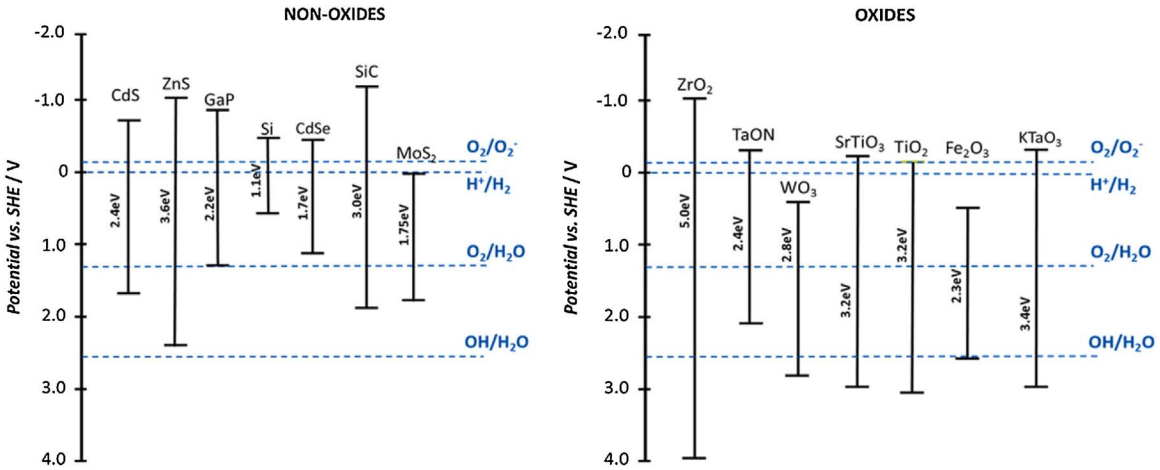

Fig. 6. The band gaps of non-oxide photocatalysts (left) and oxide photocatalysts at a pH of 7 (right) [19,96–98]. (Shaham-Waldmann & Paz, *Materials Science in Semiconductor Processing*, 72–80 (2016) 42). Copyright 2016, reprinted with permission from Elsevier.

atmosphere; purity of raw materials; chemical, microstructural and thermal homogeneity during heating; particle and agglomerate size distribution; grain and agglomerate morphology [18]. While P25 is suitable reference for photocatalysis which is activated by UV light, it is not suitable to act as a reference under visible light due its low activity under visible light, Fig. 3 [19]. As of yet, there is no standard reference material for visible light photoactivity for comparing to novel work.

Of course, another method for tailoring the phase mixture of TiO_2 is

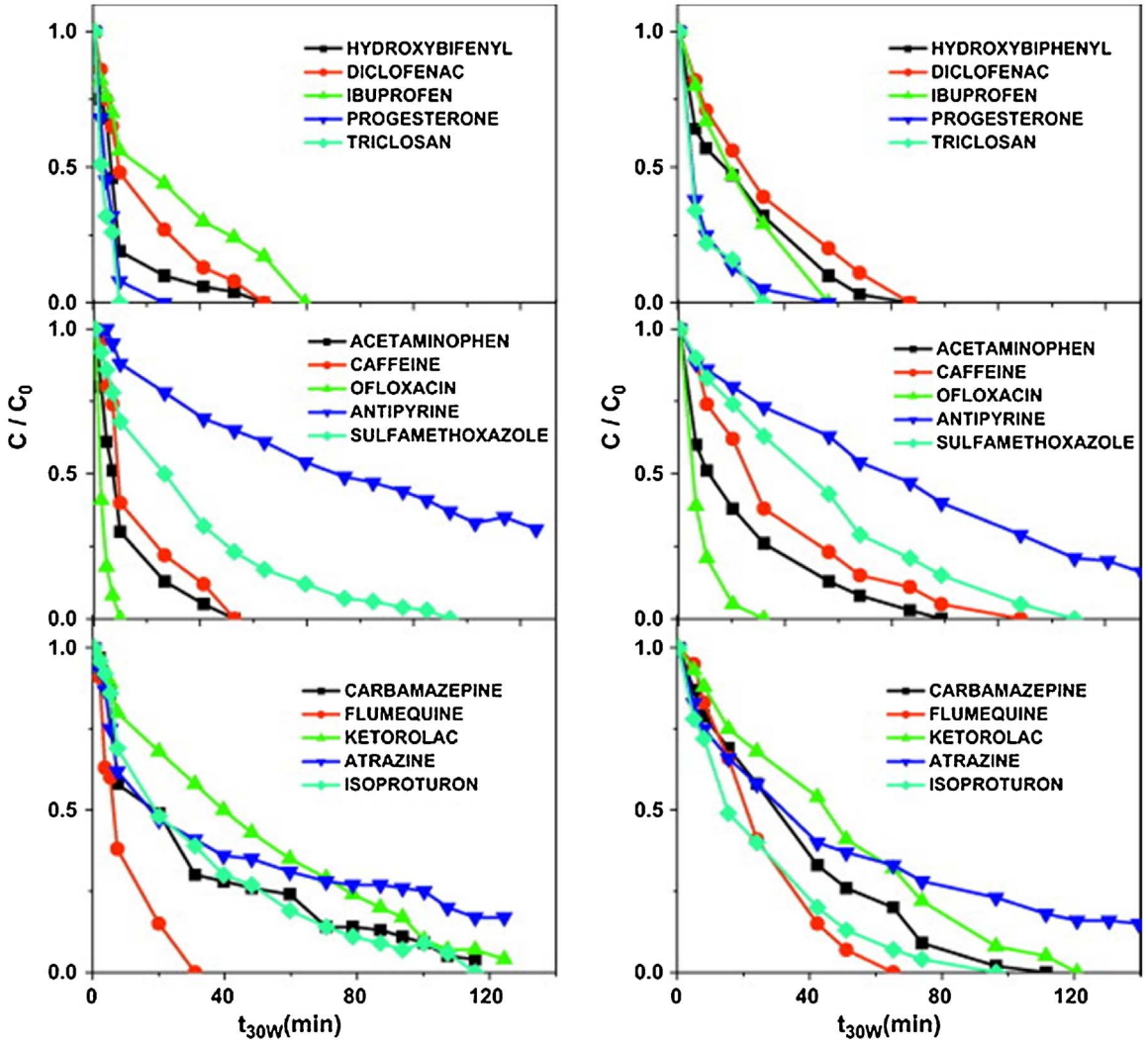

Fig. 7. Photocatalytic degradation of 15 emerging contaminants after the 1st cycle (left) and after the 5th cycle (right) [149]. (Miranda-García et al., *Applied Catalysis B: Environmental*, 294–301 (2011) 103). Copyright 2011, reprinted with permission from Elsevier.

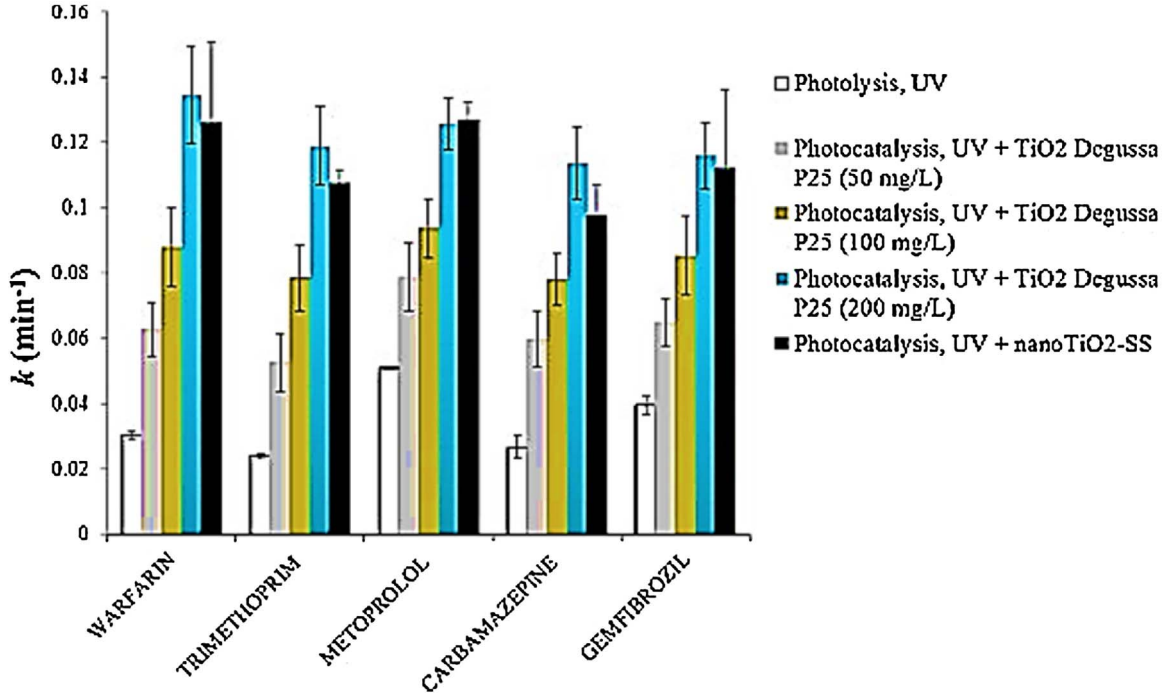

Fig. 8. Photocatalysis investigation of nano-titania compared to the photolysis and to Degussa P25 for the removal of target emerging pollutants (Warfarin, Trimethoprim, Metoprolol, Carbamazepine, Gemfibrozil,) in groundwater [150]. (Murgolo et al., *Chem. Eng. J.*, 72–80 (2016) 42). Copyright 2016, reprinted with permission from Elsevier.

the use of dopants, chemical modifiers and chemical additives. There have been thousands of compounds that have been 'doped' onto TiO_2 for this purpose [19,25]. These can be non-metal dopants (such as carbon [50,52,75–77], nitrogen [78–82], sulphur [45,60,83,84] and fluorine [85–87]) or metal dopants (such as iron [83,88], silver [36,89], chromium [90] and manganese [91,92]). When a 'dopant' is used, it can change the samples properties including the structure and could lead to the degradation of the photocatalytic activity. It can also lead to the improvement of photocatalysis by narrowing the band gap between the valance and conduction band, Fig. 3 [93].

The narrowing of the band gap between the valance band (O 2*p*) and conduction band (Ti 3*d*) occurs when dopant is used on TiO_2. The dopant introduces a new occupied orbital between the VB and the CB [24,26,94]. An example of this is when nitrogen and sulphur is used as co-dopants (Figs. 4 and 5) [24,26,94]. The N 2*p* orbital of nitrogen is used as a mid-band gap orbital for the electrons in the valance band. The electrons now require less energy in order to be excited enough in the mid-band gap orbital to reach the conduction band. When all the

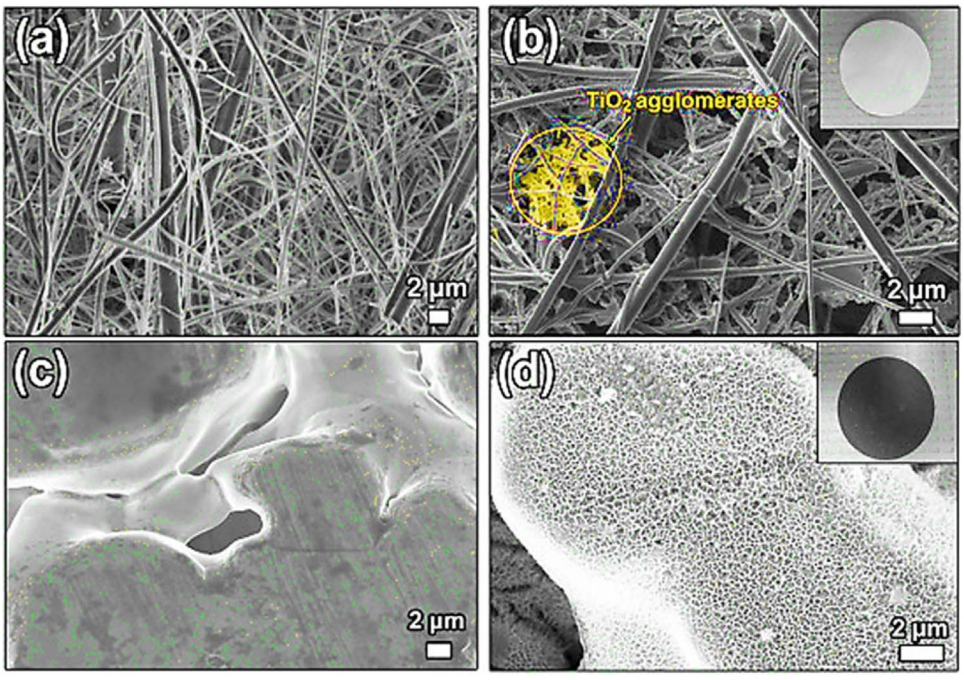

Fig. 9. SEM images of (a) raw quartz fiber filters; (b) TiO_2 coated on quartz filters (QFT); (c) raw PTi sheets; and (d) self-assembled TiO_2 on PTi sheets (PTT) [151]. (Arlso et al., *Water Research*, 351–361 (2016) 101). Copyright 2016, reprinted with permission from Elsevier.

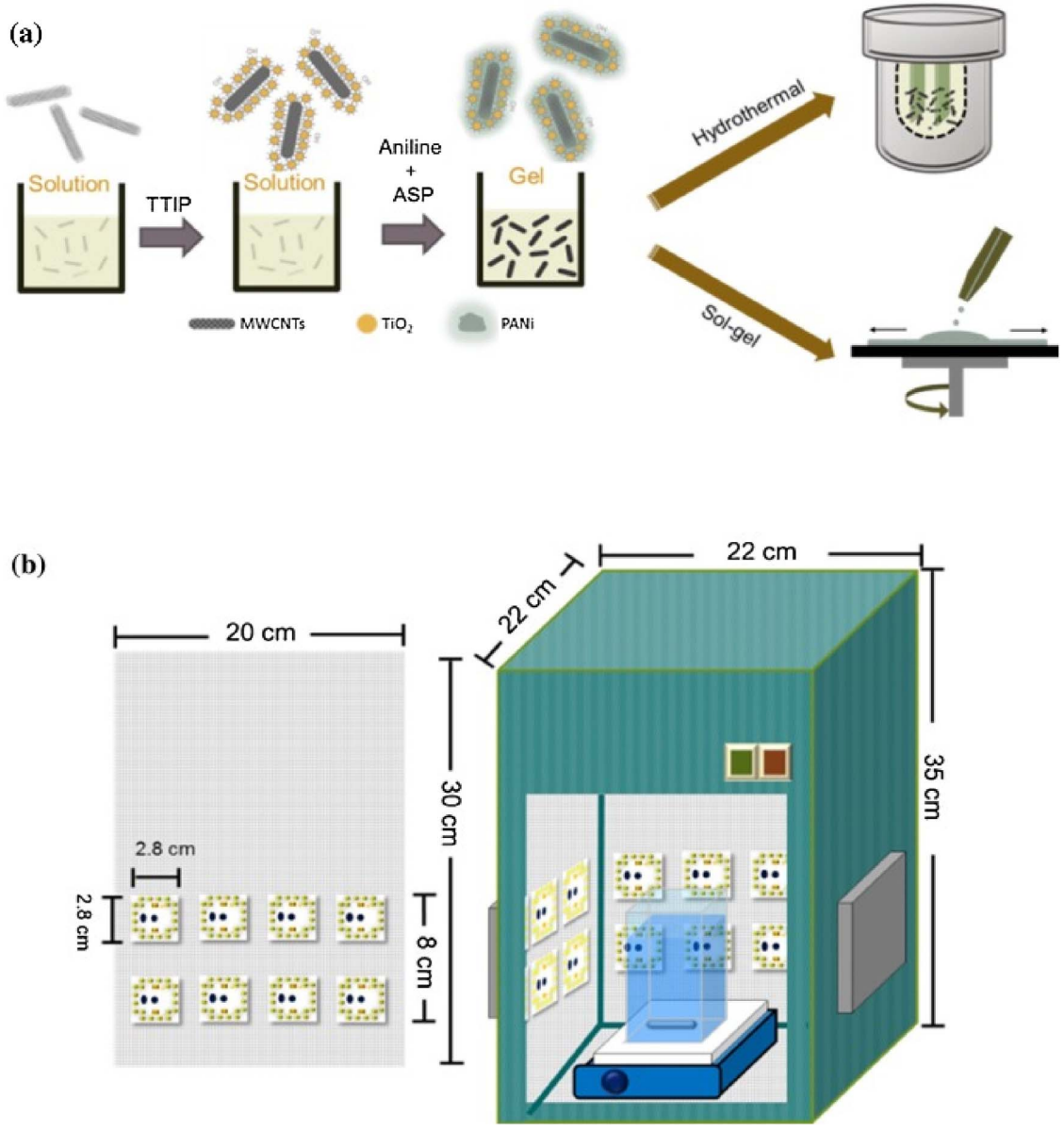

Fig. 10. (a) The preparation process of photocatalysts; and (b) A schematic diagram of photoreactor [168]. (Hung, et al., *J Hazard Mater*, 243–253 (2017) 322). Copyright 2017, reprinted with permission from Elsevier.

electrons have left the valance band, there is a positive hole left in the VB and the reaction occurs as described above [24,26,94]. The rate constants calculated for this doped-TiO2 and control titania both calcined at 600 °C, and commercial sample (Degussa P-25) are 0.0323, 0.0163, and 0.004 min^{-1}, respectively [95].

3. Novel photocatalysts

There has been a growing importance in the investigation of photocatalysts other than TiO_2, for example ZnO, ZnS, ZrO_2, semiconductor-graphene, perovskites, MoS_2, WO_3, CdS and Fe_2O_3 [19,96–103]. These photocatalysts were originally developed for the photocatalytic splitting of water, they are also being used for water/air treatment [19]. Both applications follow the same general method as described above there are a few differences which include the amount of electrons transferred, the amount of minimum energy required for the process to be induced and if the process is endothermic or exothermic. Paslernak et al. (2013) extensively compares and contrasts the two applications [104]. With the vast amount of studies looking at non TiO_2 photocatalysts, they have been divided into two categories; oxide photocatalysts and non-oxide photocatalysts (see Fig. 6). One difference between the two is that the oxide photocatalysts valance and conduction bands are affected by changes in the pH, whereas changes in pH in non-oxide photocatalysts as little or no effect on the valance and conduction bands.

Composites of two different photocatalysts has also recently gained interest [19]. The aim of this is to form hetero-junctions between the photocatalysts. These hetero-junctions will mean that the energy adsorbed by the first photocatalyst is transferred to the second photocatalyst [19]. This method causes the charge separation to increase and have a significant impact on the rate of degradation [19,65].

One example of photocatalyst that has gained significant interest is zinc oxide, this is due to it being inexpensive and having a similar photodegradation mechanism as TiO_2 [105–111]. Tian et al. [107]

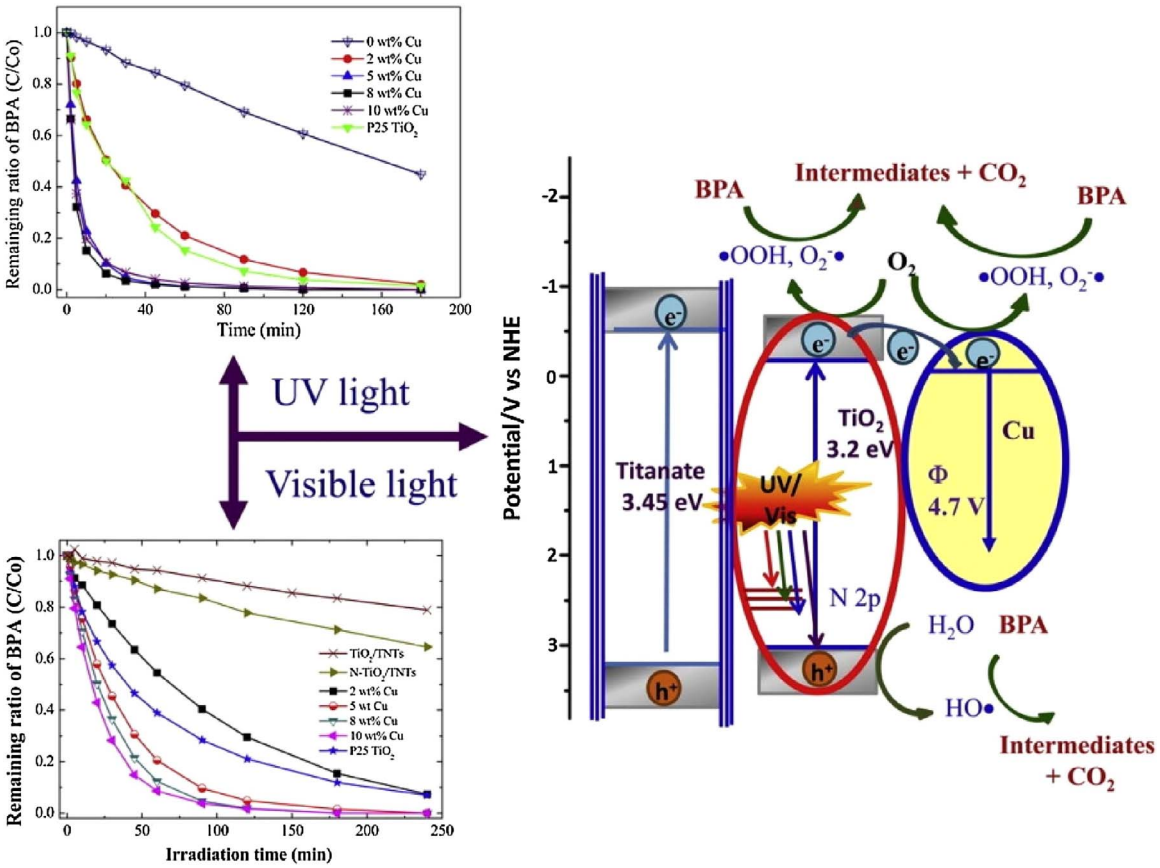

Fig. 11. Scheme showing photodegradation of BPA by Cu-deposited N-TiO_2/TNT nanocomposites under UV and visible light irradiations with proposed mechanism for photodegradation [169]. (Doong & Liao, *Sep Purif. Technol.*, 403–411 (2017) 179). Copyright 2017, reprinted with permission from Elsevier.

examined ZnO photodegradation of methylene orange in comparison to Degussa P25 TiO_2 when both were calcined at 600 °C. The study showed that the rate of degradation ZnO is significantly higher (4 times) than that of P25 [107]. As with TiO_2, there have been a number of studies that have examined 'doped' zinc oxide photocatalyst [105,108–110]. Dopants such as graphite-like C_3N_4, silver, chromium, aluminium, tin, cobalt and reduced graphene oxide have been examined with ZnO [105,108–110,112–114]. All these studies reported an enhancement in photocatalytic activity when compared with the ZnO control and a stable photocatalyst, for example Wang et al. [108] found that including a graphite-like C_3N_4 dopant improve the UV light photoactivity by 5 times [105,108–110,112–114]. Bai et al. [105] found that a ZnO_{1-x}/graphene composite enhanced the UV and the visible light photocatalytic activity, by 1.2 and 4.6 times respectively [105]. There has also been some interest into several other photocatalysts. Cadmium sulphide (CdS) has been examined as a photocatalyst [115–129], with a number of studies focusing on the production of hydrogen initiated with visible light [115,117,118,122,124]. Doped samples include ZnS-CuS-CdS, carbon spheres/CdS, *g*-C_3N_4-Au-CdS, ZnS-WS_2-CdS, C_3N_4-CdS and Pd-Cr_2O_3-CdS [115–117,120,123]. There has also been numerous studies into Zinc sulphide (ZnS) for applications such as hydrogen production and the degradation of chemicals and dyes (*e.g.* Rh B and metronidazole) [99,100,115,117,130–138].

4. Photocatalysts for water and wastewater treatment

Fresh water resources such as lakes, rivers and ground water are contaminated with a variety of organic, inorganic and microbial pollutants. Organic contaminants include industrial and agricultural chemicals; pharmaceuticals and personal care products [50]. Among these contaminants pharmaceuticals are of particular concern because they alter the metabolic activity of the living biota and could cause serious biochemical changes [139–141]. In addition, water contaminated with antibiotics and microbes lead to the emergence of antibiotic resistant bacteria posing severe threat to human health [142]. More than 200 diverse kinds of pharmaceutical chemicals are reported worldwide in different river systems [143]. Effluent from waste water treatment plants is regarded as the primary source of these pollutants [139,144–146]. Moreover the suspended particles and sludge generated in WWTPs are concentrated with contaminants and directly applied in agricultural fields as manures [139]. These facts reveal the inefficiency of conventional water treatment methods those employed in WWTPs and the need to opt for advanced water treatment technology such as TiO_2 photocatalysis.

TiO_2 photocatalysis has emerged as a promising water and waste water treatment technology. UV/TiO_2 photocatalysis was evaluated for the simultaneous degradation of five different contaminants such as 1,4 dioxane, n-nitrosodimethylamine (NDMA), tris-2-chloroethyl phosphate (TCEP), gemfibrozil, and 17β estradiol [147]. Under optimized conditions, pH 5.0 and TiO_2 dosage of 1.5 g L^{-1} 77% 1,4 dioxane, 92% for NDMA, 45% TCEP, 95% gemfibrozil and 93% 17β estradiol was degraded within 30 min. Interestingly relatively less water soluble compounds (gemfibrozil and 17β estradiol) were degraded faster than the other contaminants examined [147]. Quite different from the usual studies that employ single contaminant to evaluate TiO_2 photocatalysis, Pino et al., studied the simultaneous degradation of two phenolic pollutants 4-CP and 2,6-DCP to understand TiO_2 catalysis in competitive conditions. The study concluded that apart from active sites on the

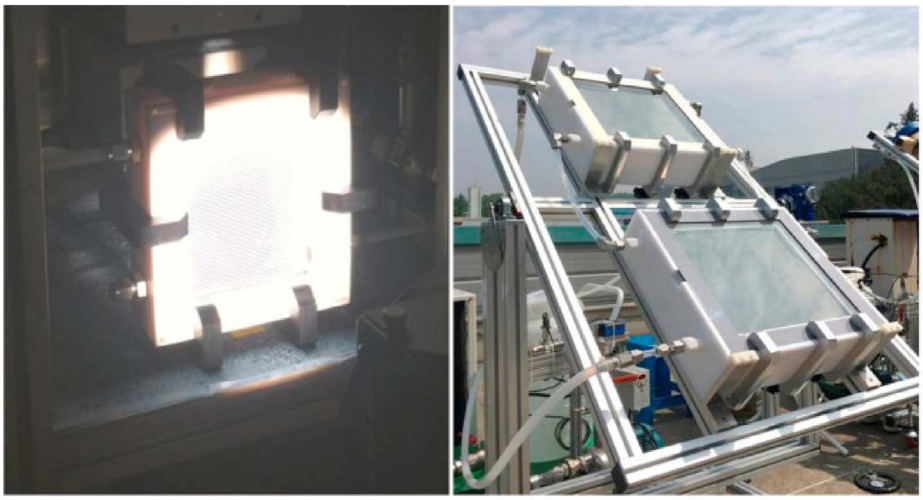

(a)

(b)

Fig. 12. Photographs of photocatalytic reactors including nanotubular TiO2 (NTT); (a) small (left) and scale-up (right) flat-type reactor, (b) small (left) and scale-up (right) rotating-type reactor [171]. (Kim, et al., *J Hazard Mater*, 21–32 (2017) 336). Copyright 2017, reprinted with permission from Elsevier.

surface, other parameters such as initial pH, initial concentration, light intensity, the interplay of several parameters related to the surface properties, phenol structure and the adsorption effect of intermediate products also affect the performance of the system [148]. In view of operational feasibility, immobilized TiO_2 is more preferred than TiO_2 suspended in the form of slurry. TiO_2 immobilised on glass substrate was successfully applied for the solar photocatalytic degradation of 15 emerging contaminants (acetaminophen, antipyrine, atrazine, carbamazepine, diclofenac, flumequine, hydroxybiphenyl, ibuprofen, isoproturon, ketorolac, ofloxacin, progesterone, sulfamethoxazole and triclosan) present in simulated and real Municipal Wastewater Treatment Plant (MWTP) effluents at environmentally relevant concentrations in a pilot compound parabolic collector. Significant (~85%) removal of these contaminants was achieved within 120 min, revealing the potential application of this technology for waste water treatment plant effluents Fig. 7 [149].

In another recent study, TiO_2 deposited as film on a stainless steel mesh by Chemical Vapour Deposition (CVD) technique was evaluated for the photocatalytic degradation of a mixture of emerging contaminants such as Warfarin, Trimethoprim, Metoprolol, Carbamazepine, Gemfibrozil, Terbutaline, Iopromide, 2,4 Dihydroxybenzophenone, Perfluorooctanesulfonic acid, and Perfluorooctanoic acid in real groundwater. The results revealed that immobilized TiO_2 on stainless steel mesh performed better than Degussa P25 in eliminating these contaminants (Fig. 8). Moreover different toxicological assays such as Vibrio fischeriacute toxicity test, Daphnia magna acute toxicity test, Green alga Selenastrum capricornutum test, AMES Fluctuation test and Fish Embryo Acute Toxicity Test revealed the significant reduction in the toxicity of the treated water [150].

Immobilized TiO_2 (Fig. 9) in the form of quartz fiber filters (QFT) and porous titanium sheets (PTT) were applied to treat waste water contaminated with pharmaceuticals such as Carbamazepine, Venlafaxine, Fluoxetine, Atenolol, Sulfamethoxazole, Ibuprofen, Atorvastatin, and Naproxen, and personal care products such as Triclosan, Triclocarban and the metabolites of these contaminants including Carbamazepine-10,11-epoxide, Norfluoxetine, p-hydroxy atorvastatin, o-hydroxy atorvastatin [151]. Notably, at pH condition of 4.5-5, QFT membranes are negatively charged whereas while PTT membranes are

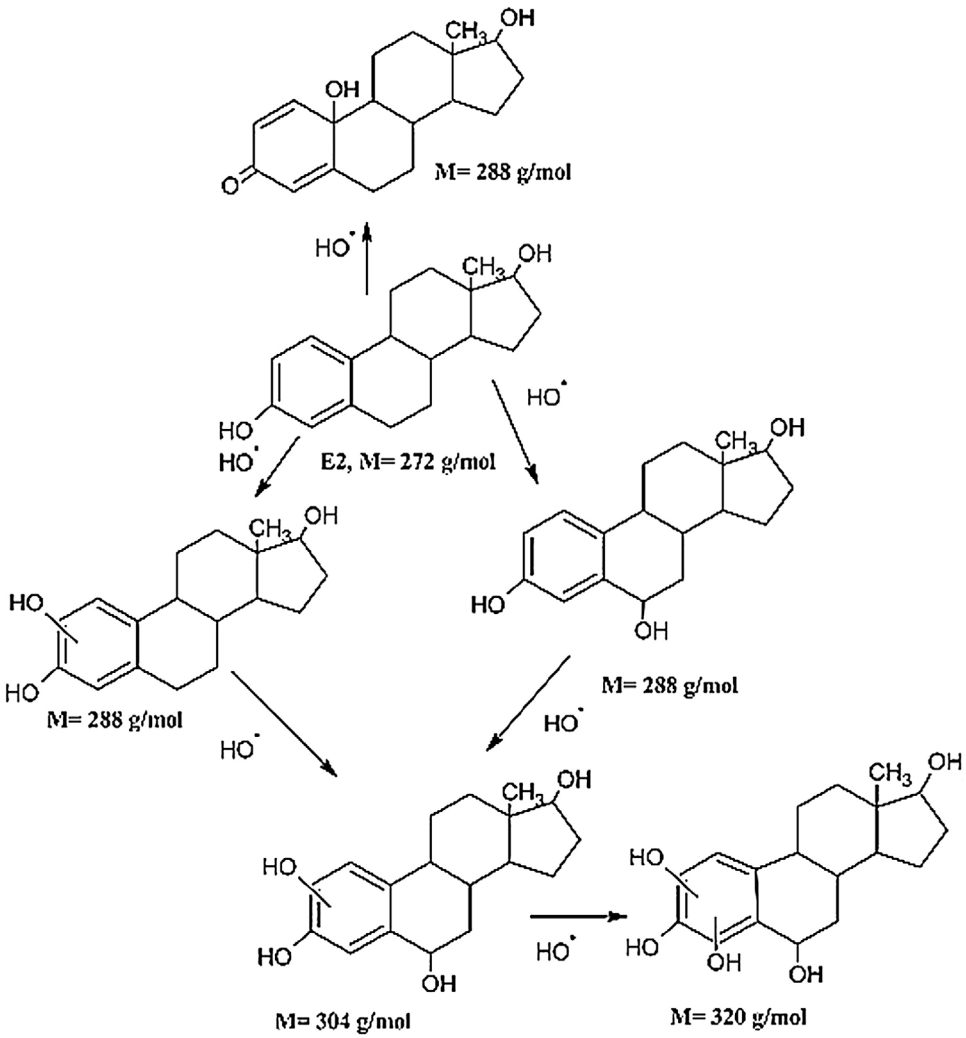

Fig. 13. Photocatalytic degradation of mechanism 17β-estradiol [173]. (Maroga Mboula et al., *Applied Catalysis B: Environmental*, 437–444 (2015) 162). Copyright 2015, reprinted with permission from Elsevier.

positively charged. Consequently, the results revealed interactions between charged contaminants and membranes played a important role in the degradation. QFT membrane was effective in removal of cationic compounds while PTT was effective in removal of anionic contaminants. Nevertheless, both forms of immobilized TiO_2 materials are reusable after heat treatment and useful for effective treatment of contaminants of emerging concern [151]. TiO_2 anatase phase nanobelts of 10 μ length and 30–100 nm was able to degrade different organic contaminants such as dye (malachite green), three pharmaceuticals (naproxen, carbamazepine) and personal care product theophylline [152]. Natural organic matter (NOM) that co-exists with real water matrices can adsorb to TiO_2 nanoparticles causing agglomeration and subsequent reduction in the catalytic efficiency [153–157]. Moreover, NOM effectively scavenge photogenerated holes and radicals and compete for ROS generated in TiO_2 photocatalysis [153–157]. However, Long et al. recently demonstrated that the inhibitory effect of NOM during photocatalytic water treatment can be reduced by anchoring phosphate anions on TiO_2 surfaces [158]. The phosphate anions play a beneficial role by decreasing HA adsorption thereby mitigating electron–hole recombination induced by adsorption of HA [158]. All these studies demonstrate the superior ability of TiO_2 photocatalysis to degrade a diverse class of organic contaminants that are not removed by traditional water treatment methods.

Besides organic contaminants, toxic inorganics can also be eliminated by TiO_2 photocatalysis. TiO_2 photocatalysis has been considered as an efficient method for remediation of arsenite and toxic hexavalent chromium contaminated waste waters [3,4,16,17,159–163]. Oxidation of As(III) to As(V) is mediated by the electron transfer between As(III) and the photogenerated positive hole [161]. As alternate approach, simultaneous UV-catalyzed oxidation–coagulation treatment of arsenite contaminated waste water with titanium sulphate effectively oxidized toxic As(III) to non-toxic As(V) in pH range 4–6 [160]. TiO_2 nanotubes formed on titanium mesh substrates fabricated on a rotating disc reactor were able to simultaneously reduce toxic hexavalent chromium to

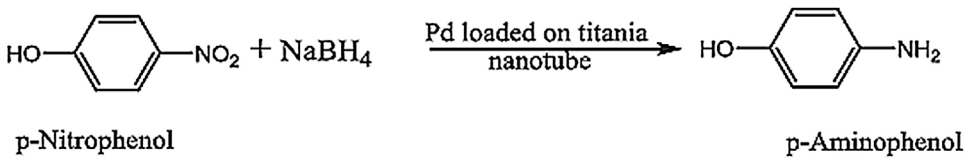

Fig. 14. Photoreduction of 4- Nitrophenol to a valuable chemical 4–aminophenol [178]. (Kalarivalappil, et al., *Catalysis Letters*, 474–482 (2016) 146). Copyright 2016, reprinted with permission from Elsevier.

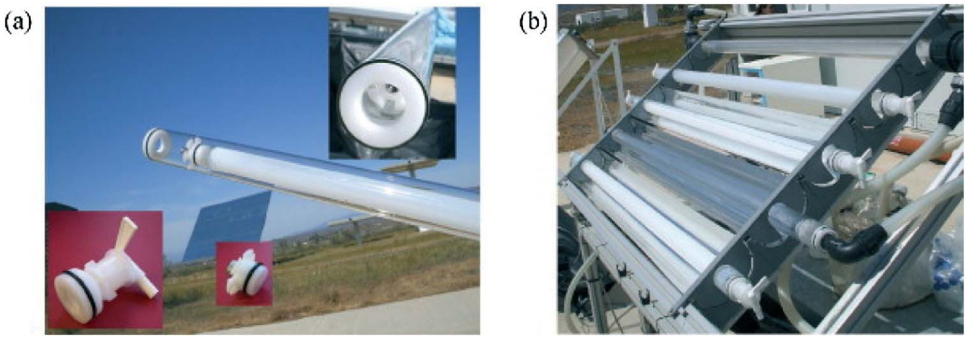

Fig. 15. CPC solar pilot plant using titania coated glass tubes for solar photocatalytic degradation experiments. Reprinted from Alrousan et al., Solar photocatalytic disinfection of water with immobilised titanium dioxide in re-circulating flow CPC reactors, Appl. Catal., B, 2012, 128, 126–134. Copyright (2012), with permission from Elsevier. [182].

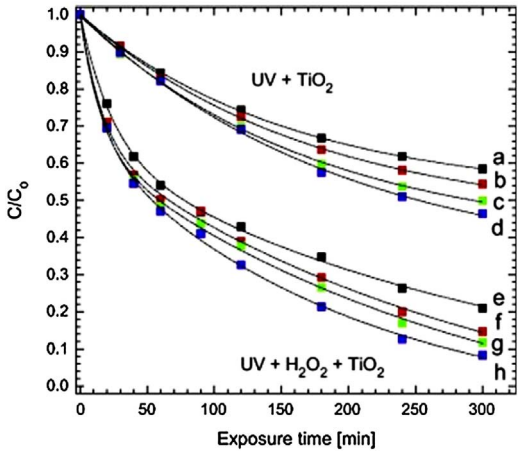

Fig. 16. Carbaryl pesticide degradation under experimental conditions of UV + TiO_2 (curves a–e and UV + H_2O_2 + TiO_2 (curves 5e–h) as function of exposure time for different solar concentration ratios of CPC solar collectors: (a) 1, (b) 1.5, (c) 1.75 and (d) 2 suns. Initial carbaryl concentration is C_o = 50 mg/l. (Salgado-Transito et al., *Solar Energy*, 537–551 (2015) 115). Copyright 2015, reprinted with permission from Elsevier.

non-toxic trivalent chromium as well as oxidised endocrine disrupting chemicals under solar irradiation [164].

5. Photocatalysts for endocrine disrupters and pesticides

The endocrine system is the collection of glands such as pituitary gland, thyroid gland, parathyroid glands, adrenal glands, pancreas, ovaries (in females) and testicles (in males) that produce hormones involved in the regulation of metabolism, growth and development, function, reproduction, sleep, and mood. Endocrine disrupting compounds (EDCs) are a hazardous group of chemicals that cause undesirable change in the biochemical activity of endocrine system, leading to serious health consequences. Importantly, these hazardous chemicals are being discharged in to water systems by various human activities causing serious health and environmental concern. EDS are broadly distinguished in to: pesticides (e.g., DDT, dichlorodiphenyltrichloroethane); halogenated and aromatic compounds (e.g., dioxins); heavy metals (e.g., cadmium); alkyl phenols (e.g., bisphenol A); phthalates (e.g., dibutyl phthalate); steroids (e.g., genistein); and preservatives (e.g., parabens) [7,140,165,166].

Photocatalytic degradation of EDCs is a promising approach to remove a variety of EDCs from contaminated water. A comprehensive account on progress in this field has been recently reviewed [7,140,166]. Photocatalysis mediated by metal oxide nanomaterials, such as TiO_2, ZnO, WO_3, ZnS, SnO_2 and Fe_2O_3 and Bi_2WO_6, were useful to degrade endocrine disrupting contaminants [7,140,166,167]. Desirable attributes such as high effeciency, chemical and photo stability, low cost, commercial availability and biocompatibility of TiO_2 makes it a most preferred and actively studied photocatalyst to eliminate EDCs [166].

Hung et al., fabricated a series of glass surface immobilised TiO_2/polyaniline/carbon nanotube (PANi/CNT/TiO_2) *via* two strategies, hydrothermal synthesis and a sol–gel hydrolysis, and studied the degradation of a model EDC Diethyl phthalate (DEP) (Fig. 10). In this study, a light emitting diode (LED) based simulated sunlight photoreactor was established to investigate the solar photocatalysis of DEP [168]. CNTs prevented the quick recombination of electron-hole pairs and PANi enhanced electron conductivity and also increased the absorption wavelength of photocatalyst to visible light region. The study demonstrated the successful degradation of DEP by hydroxyl radicals generated using immobilized PANi/CNT/TiO_2 photocatalyst [168]. With anatase TiO_2 nanoparticles as the raw materials, Doong et. al., developed a Cu-deposited N-TiO_2/titanate nanotubes *via* microwave-assisted hydrothermal method [169]. The study demonstrated the enhanced photocatalytic degradation of EDC bisphenol A (BPA) when compared to commercial P25 under both UV and visible light irradiations (Fig. 11).

XRD and XPS results revealed Cu species present in the form of Cu_0 and N atoms in the TiO_2 composite mainly in the forms of O-Ti-N and Ti-O-N. BPA degradation rate correlated with Cu mass loading. The authors propose that the presence of Cu_0 caused formation of Schottky barrier, and enhanced the photodegradation rate of BPA [169]. A novel interfaced anatase-rutile catalysts produced by thermohydrolysis and also tuned by Sn(IV) was prepared to investigate the photocatalytic degradation of an artificial sweetener Saccharin (SAC) and EDC BPA, as model contaminants [170]. The results revealed that the efficiency of this novel catalyst is same for removing SAC or BPA degradation. Moreover, the catalyst was reusable and showed 70% removal of contaminant after 3 successive runs. The effect of ultra sound treatment on catalytic performance was also investigated by treating the reactant mixture with ultra sound, at the beginning of each cycle for 10 min. However, ultra sound treatment had no significant effect on treatment efficiency.

Kim et al., investigated the removal efficiencies of mixed EDCs, in two different scales of rotating and flat-type TiO_2 photocatalytic reactors (Fig. 12) and compared the reactor performances on removal efficiency [171]. Several operational parameters such as hydraulic retention time (HRT), initial concentrations, single and mixed compounds, UV intensities, and dissolved oxygen, effect of the average solar UVintensities, effect of Cr(VI), pH on EDC-removal process were demonstrated under outdoor solar irradiation. The results revealed that for the both photocatalytic reactors (rotating and flat-type) decrease in HRT increased degradation efficiency because of increased mass transfer [171].

Molecularly imprinted polymers modified silver nanoparticle-TiO_2 nanotubes (MIP-Ag/TiO_2 NTs) were investigated for photocatalytic decomposition of an EDC, perfluorooctanoic acid (PFOA) in aqueous solution [172]. The modified MIP-Ag/TiO_2 NTs showed encouraging

Fig. 17. 1: In situ generated TiO_2 over zeolitic supports for degradation of pesticide dichlorvos (left). 2: Degradation and mineralization degree of dichlorvos as a function of the number of cycles of use. [187] (Gomez et al., *Applied Catalysis B: Environmental*, 167–173 (2015) 162). Copyright 2015, reprinted with permission from Elsevier.

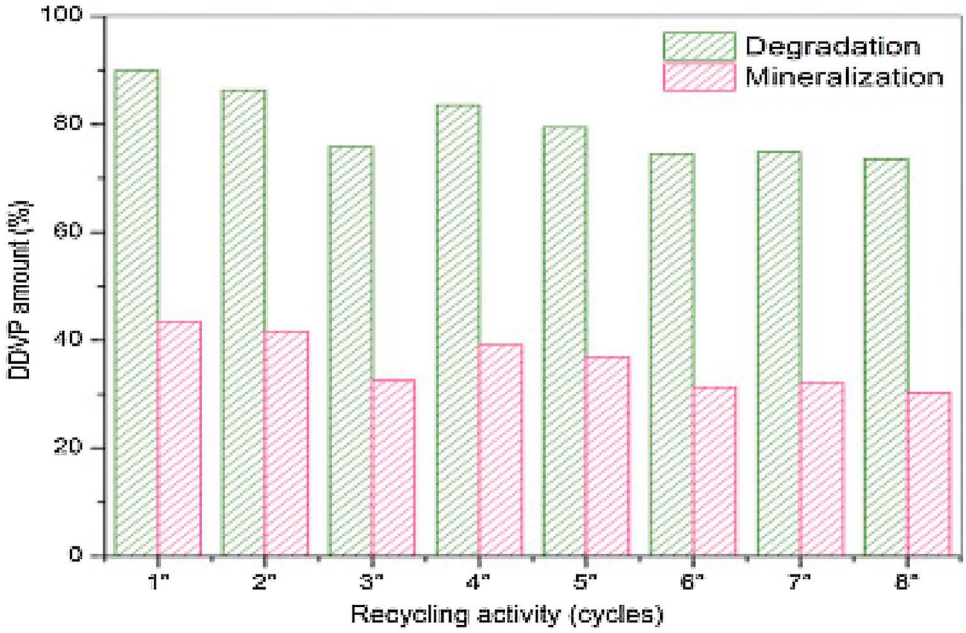

results. About 91% of PFOA was degraded after 8 h reaction. Shorter-chain PFCs were identified as main degradation products, and the PFOA degradation mechanism and pathway were proposed. However, it is important to determine the residual toxicity of the degradation intermediates because these intermediate species may also exert endocrine disrupting activity [172]. This important information was clearly exhibited in a study by Mboula et al., that examined the photocatalytic degradation of 17β-estradiol using three types of TiO_2 materials such as nanocrystalline TiO_2; nitrogen-modified TiO_2; and reduced graphene oxide-TiO_2 composite and also assessed the toxicity post treatment. The results revealed that even after degradation of 17β-estradiol to below its detection limits, residual estrogenic activity still persisted revealing the complications associated with treatment of challenging contaminants such as endocrine disrupters (Fig. 13) [173].

Methylparaben is a widely spread and a highly recalcitrant EDC. Photocatalytic degradation of methylparaben by TiO_2 suspensions under different light irradiations (UV-A, UV-C and Visible) were investigated [174]. The results show UVC- TiO_2 photocatalysis as highly efficient for the degradation and mineralization of methylparaben. The acute toxicity of residual intermediates performed with *Artemia franciscana* showed a significant decrease of toxicity after photocatalytic degradation of MEP [174]. In view of large scale applications, a submerged membrane TiO_2 photocatalytic reactor was evaluated for the removal of 17β-estradiol in presence of a representative natural organic matter, humic acid. Long term assessment of the membrane properties revealed that aged TiO_2 caused higher trans-membrane pressure and poor removal of humic acid. As a consequence the performance of this membrane reactor decreased with time [175]. A solar simulator irradiated TiO_2 and TiO_2/WO_3 electrodes degraded 17-α-ethinylestradiol effectively both by photocatalysis and electrochemically assisted

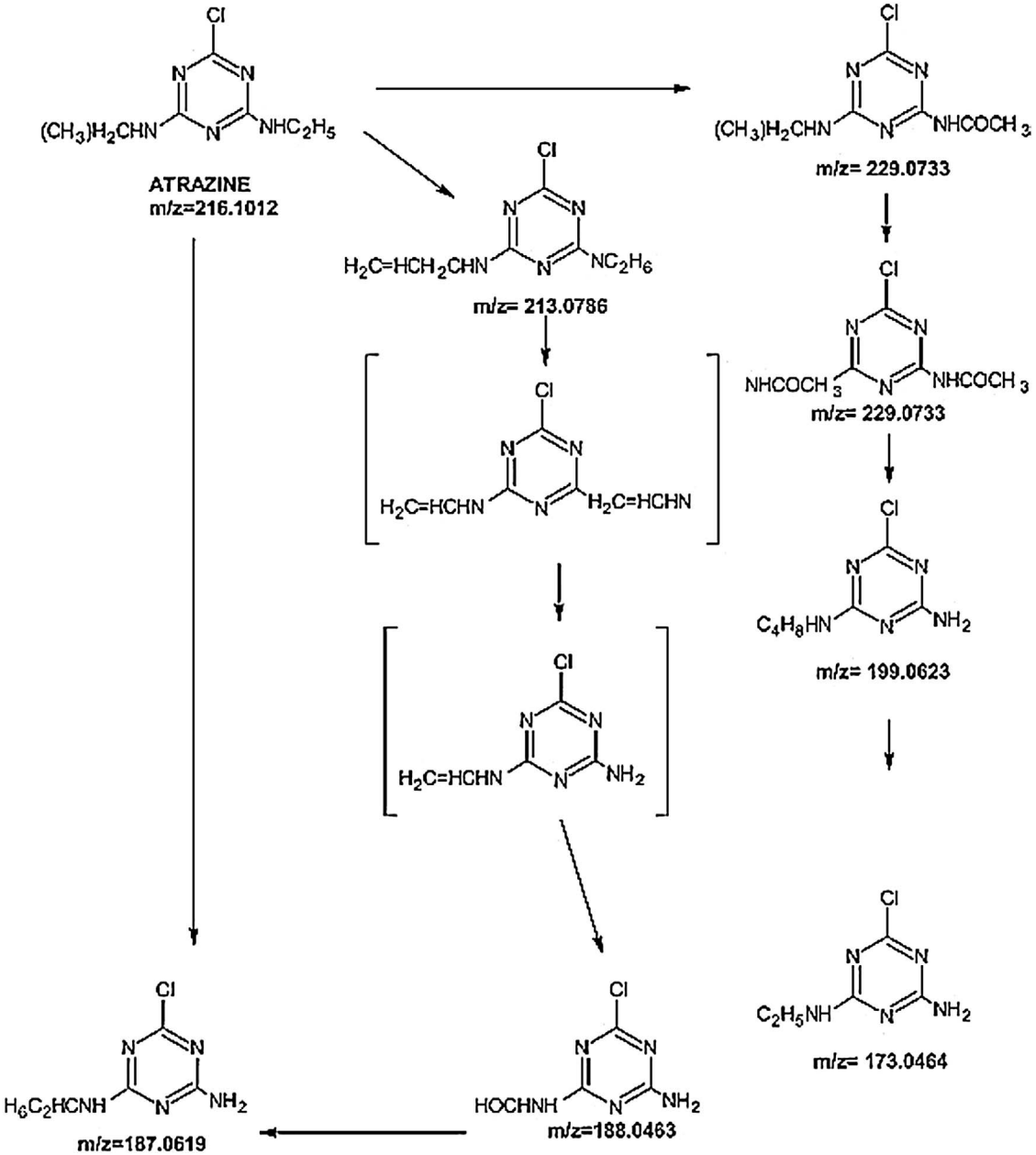

Fig. 18. Photocatalytic degradation of atrazine by TiO_2 materials supported on phosphorescent zinc sulphide microparticles under UVA irradiation [188]. (Sacco et al., *Applied Catalysis B: Environmental*, 462–474 (2015) 164). Copyright 2015, reprinted with permission from Elsevier.

photocatalysis. Incorporation of WO_3 in TiO_2, was useful to prevent the recombination of charge carriers resulting in enhanced light utilization to realise effective contaminant degradation [176]. 4- Nitrophenol, a common contaminant in domestic and industrial effluents is also an endocrine disruptor. Silver deposited TiO_2 was highly efficient in rapid photoreduction of 4- Nitrophenol (or *p*-Nitrophenol) to a valuable chemical 4–aminophenol (*p*-aminophenol) [177]. In a similar study Kalarivalappil et al., investigated the impact of pd loaded titania nanotubes for the photoreduction of 4- Nitrophenol to a valuable chemical 4–aminophenol (Fig. 14) [178]. The 1.0 mol% Pd doped TiO_2 nanotubes showed optimum photocatalytic activity.

The above examples clearly outline the challenges in photocatalytic treatment of endocrine disrupters and the need to develop many efficient strategies for abatement of these contaminants. Assessment of residual activity post treatment method is important in absolute evaluation of the treatment method.

Pesticides or organic chemicals employed to kill pests that affect the crop productivity are inevitably useful for mankind. However, due to excessive usage and poor management these chemicals contaminate fresh water ecosystems via agricultural runoff and persist for a very long period in soil and water bodies [179,180]. Most of these agrochemicals are hydrophobic in nature thus posing a particular challenge in aqueous oxidative degradation reactions. Photocatalytic degradation of pesticides using TiO_2 has been regarded as an effective approach to alleviate pesticide pollution. Carbamates type pesticides such as Oxamyl and Methomyl adsorbed well on TiO_2 surfaces which on irradiation was efficiently mineralized in to CO_2, SO_4^{2-}, NH_4^+, and NO_3^- ions [181]. Pesticides such as Thiabendazole, imazalil and acetamiprid were effectively degraded using an immobilized solar TiO_2 photocatalytic reactor. A CPC solar pilot plant using TiO_2 glass tubes for solar photocatalytic degradation experiments is given in Fig. 15.

Moreover, the TiO_2 coated glass beads were recyclable for at least

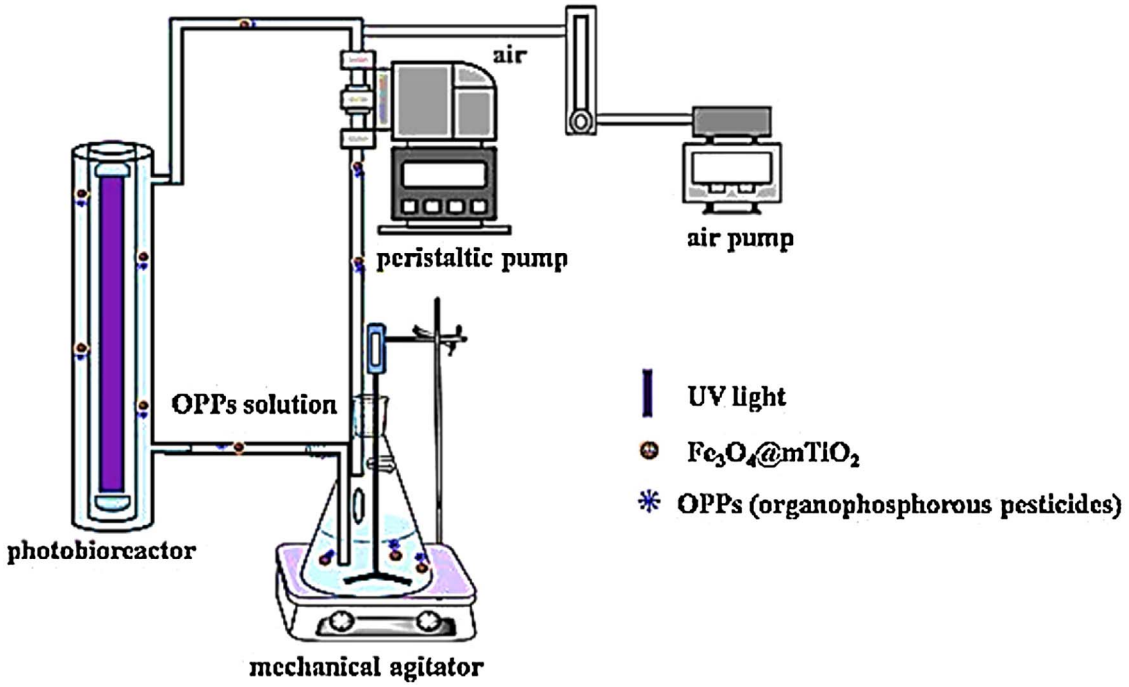

Fig. 19. Photoreactor used for the photocatalytic decomposition of acephate, omethoate, and methyl parathion [191]. (Zheng et al., *Journal of Hazardous Materials*, 11–22 (2016) 315). Copyright 2016, reprinted with permission from Elsevier.

five times without loss of activity [183]. Chlorpyrifos, lambda-cyhalothrin, and diazinon were effectively degraded by solar TiO_2 photocatalysis. UVC/TiO_2 photocatalysis was more effective than UVC photolysis alone in degradation and mineralization of pesticide diazinon. Notably, the presence of anions had a positive effect on UVC photolysis while negatively affected TiO_2 photocatalysis [184]. A specially designed multiple compound parabolic concentrators showed notable improvement in solar TiO_2 photocatalytic degradation of carbaryl pesticide. Importantly, the addition of environmentally benign oxidant hydrogenperoxide was useful to improve the overall degradation efficiency Fig. 16 [185,186].

Intense efforts on modified TiO_2 materials have shown promising results in degradation of pesticides. Zeolitic matrices supported titania showed more surface area and a lower band gap energy that were useful in effective degradation of dichlorvos (Fig. 171). Moreover, dichlorvos adsorbed well on to the zeolite matrix which also played an important role in photocatalytic degradation. The catalyst showed excellent reusability both for the degradation and mineralization of dichlorvos (Fig. 172) [187]

Nitrogen doped visible light active TiO_2 materials supported on phosphorescent zinc sulphide microparticles were employed to degrade atrazine, a highly persistent contaminant (Fig. 18). The solution pH and catalyst concentration played important role in degradation efficiency of this process [188]. Analysis of the degradation intermediates of atrazine revealed that dealkylations and alkyl chain oxidation are the key reactions of this photocatalytic system. Cyanuric acid is a common degradation intermediate produced on photocatalytic treatment of atrazine. [189,190] Importantly, cyanuric acid is resistant to hydroxyl radicals and known to persist after photocatalytic treatment. Interestingly, in the degradation of atrazine by phosphorescent zinc sulphide supported TiO_2 cyanuric acid was not produced. Moreover, dechlorination of atrazine was also not observed [188]. These findings indicate the unique degradation mechanism of this novel photocatalytic system.

The performance of a magnetically separable and reusable hybrid $Fe_3O_4/SiO_2/TiO_2$ photocatalyst was tested in a circulation type photocatalytic reactor consisting of a long glass tube around a high pressure mercury lamp emitting radiation between 330 and 390 nm (Fig. 19) [191].

Organophosphate contaminated feed solution mixed with photocatalyst was continuously stirred in a using an overhead stirrer. The solution was circulated using peristaltic pump and air pump. This novel photocatalytic system was very effective than commercial P25 TiO_2 in degradation and mineralization of pesticides such as acephate, omethoate, and methyl parathion. Among these pesticides acephate required relatively more treatment time (80 min) than omethoate, and methyl parathion (50 min) for complete degradation. The photocatalytic degradation mechanisms were dependent on the structure of these pesticides, (Fig. 20).

In case of acephate the first step was oxidation of the acetyl group while in case of Omethoate the first step was cleavage of P-S bond followed by cleavage of S-C bond. (Fig. 20) On the other hand, three different pathways were proposed for Methyl parathion degradation including the initial cleavage of the nitro-phenyl bond, P S bond, and the P O bond that connects to the aromatic ring. (Fig. 20) [191]. However all the intermediates of these pesticides were effectively degraded into small organic molecules and subsequently transformed into inorganic species resulting in the reduction of total organic carbon.

6. Anti-microbial applications of photocatalysts

There have been an extensive number of studies that have successfully used semiconductors for their anti-microbial properties [1,192–195]. As discussed above, doping is one of the methods for improving photocatalytic activity. There has been a vast number of dopants that have been examined specifically for the inactivation of bacteria, some examples include nitrogen [196], nitrogen-silver, [197,198], nitrogen-copper [51], sulfur [199], carbon [52], nickle [83], and copper [50,83]. The photocatalytic mechanism that inactivates bacteria begins with rupturing the cell membrane, this results

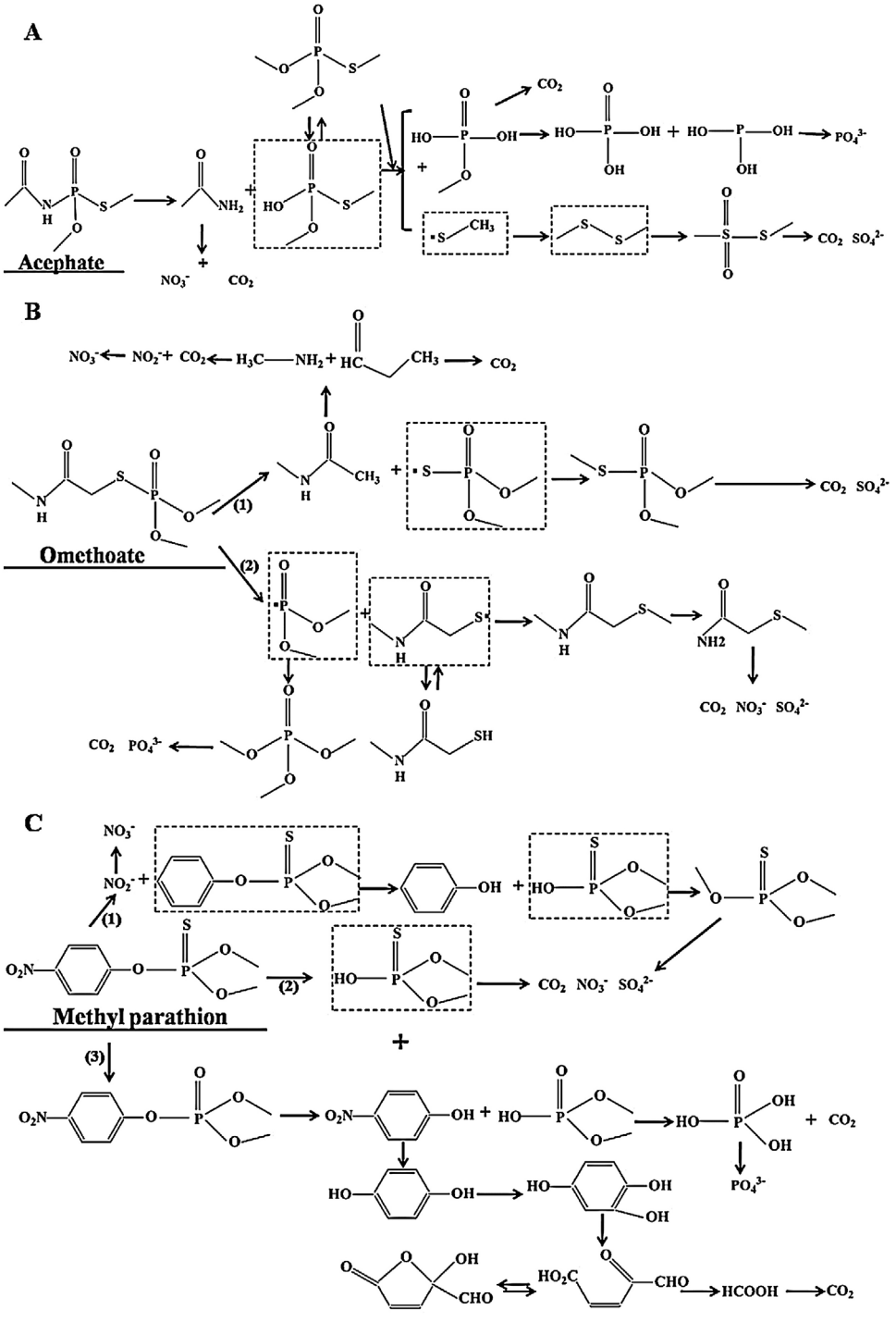

Fig. 20. Proposed photodegradation schemes of Acephate (A), Omethoate (B), and Methyl parathion (C) [191]. (Zheng et al., *Journal of Hazardous Materials*, 11–22 (2016) 315). Copyright 2016, reprinted with permission from Elsevier.

in the bacteria's internal components to leak from the areas that have been ruptured (Fig. 21) [50]. The components that have been leaked are oxidised by photocatalytic sites (Fig. 21) [50].

Pulgarin's research group have completed an extensive study on N-S doped TiO_2 and its effect on photocatalytic inactivation of *E. coli* [200–203]. Their study uses thiourea as a source of N-S for co-doping TiO_2 and for the inactivation of *E. coli* [200]. After calcination at 400 °C and 500 °C, Pulgarin's group were able to determine that varying the temperature resulted in different doping species [50]. The formation of reactive oxygen species (ROS), they concluded, is affected by the nature of the dopant used, the particle size and the surface hydroxylation [50,200–203]. From the studies it can be suggested that under visible light treatment, *E. coli* is inactivated when superoxide anion radicals (O_2^-) and singlet oxygen ($^1O_2$) are formed [50,200–203]. These are formed from electrons in nitrogen and sulfur localised states [201,202]. These samples were also examined under UV light for ROSs [203]. It was found that under UV light, it was hydroxyl radicals (OH) that was involved in the inactivation of *E. coli*. These radicals are formed on the valance band holes by the oxidation of water [50,200–203].

The use of carbon doped TiO_2 anatase-brookite heterojunctions was examined for the inactivation of *S. aureus* (Fig. 3) [52]. The use of a 80:20 (anatase: brookite) proved to be an effective method for *S. aureus*

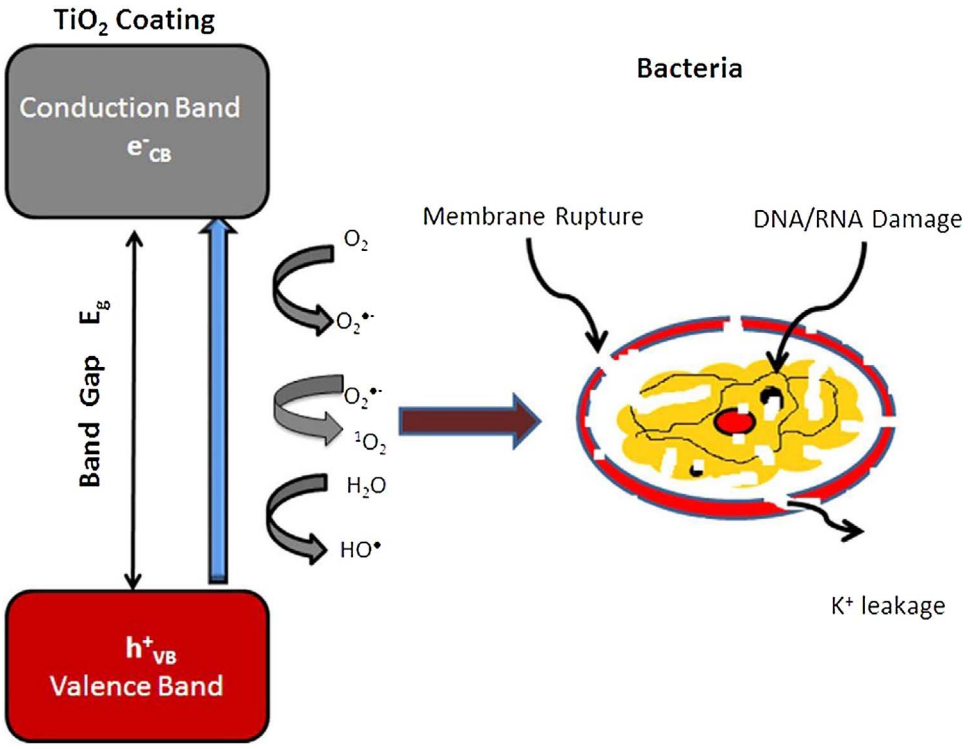

Fig. 21. Photocatalytic inactivation of bacteria [40] (Leyland et al., *Scientific Reports,* (2016), 6.). Copyright 2016, reprinted with permission from Scientific Reports.

under visible light [50,52]. There also additional energy levels formed due to the carbonate ions, this lead to a sizable band gap narrowing [50,52]. The result from this narrowing of the band gap is an significant increase in photocatalytical activity and antibacterial properties [50,52]. The decreased rate of the recombination between the electron in the conduction band and the positive hole in the valance band is what causes this increase in activity. The hydrogen peroxide (H_2O_2), which is produced as a result from surface of H_2O and OH^-, causes the formation of protonated superoxide radicals (HO_2) when reacted with OH and breaks down bacterial cells, Fig. 21.

E. coli and *S. aureus* are two of the numerous bacteria that have been studied in relation to the impact of nanotubes (NTs) for antimicrobial activity [205]. As with all other powder samples, the physical properties and the phase mixture of the NTs has a significant impact on the antimicrobial activity [50,204,206]. Garvey et al. (2016) recently completed a significant study on TiO_2 nanotubes, examining the phase transition temperature and the photocatalytic inactivation of microbes [204]. The sensitivity of the microbes while they were in the log and stationary phases was also examined during this study [204]. The effectiveness of any disinfectant is completely dependent on whether or not the cells are in the stationary or log phase and the resistant of the cells to chemical disinfection [204,205,207,208]. The main aim of this study [204] was to develop an effective method for disinfection of water during both the stationary and log phases of growth [204]. In order to show that photocatalytic activity was occurring, controls (bacteria in the absence of irradiation of light and bacteria without the NTs under UV light, 365 nm) were run for both stages of the bacteria life cycle [204]. There was no bacterial inactivation for these samples, these were used for comparison with samples that had the titania NTs present [204]. Fig. 22 shows the results of all bacteria strains examined in the log phase at various times [204]. The uncalcined and 200 °C TiO_2 NTs treated bacteria samples showed significant levels of inactivation at, all time intervals [204]. For *S. typhimurium* the NTs which was calcined at 200 °C gave a higher rate of bacterial inactivation then the uncalcined NTs (Fig. 19a) [204]. With the increase in temperature and increase percentage of rutile there was a decrease in the inactivation of bacteria. The sample that contained the highest percentage of rutile (calcined at 800 °C) showed to be the least toxic to bacteria. The NTs proved to be the most toxic to *P. aeruginosa* (Fig. 22b) at all temperatures [204]. The NTs were the least toxic to *E. coli* (Fig. 22c) across all temperatures, there was less than 1 $\log_{10}$ rate of inactivation at 600 °C and 800 °C [204]. However at lower temperatures (uncalcined and 200 °C) *E. coli* showed high levelled of inactivation (a 2.7 $\log_{10}$ reduction) [204]. As with the other bacteria, there was an increased presence of *E. coli* when there was a higher percentage of rutile present in the NTs, a result of calcination at elevated temperatures [204]. The rate of inactivation of the NTs at lower temperatures than the reference, P25 NPs [204]. When treated with NTs at temperatures between 400 and 800 °C, *P. aeruginosa* (Fig. 22b) showed results similar to P25. In comparison to this, P20 NP proved to be more toxic to *E. coli* than the NTs (Fig. 22c) [204].

7. Metal organic frame works (MOFs)

Recently, metal organic frame works (MOFs) have gained a lot of interest in photocatalytic degradation of organic contaminants [209–212]. MOFs are porous inorganic – organic hybrid materials in which metal containing nodes and organic ligands are connected *via* coordinative bonds. The availability of several organic ligands and the ability of such ligands to form coordination bond with several metal ions has resulted in a lot of interesting metal organic frameworks with important practical applications [209–212]. The unique properties of MOFs stems from the structural and chemical tunability. Zinc, copper, cobalt and iron are the most widely used metals for constructing photoactive metal organic frameworks for the degradation of organic contaminants. Readers are recommended to refer to four literature reviews are available on the photocatalytic MOFs towards water decontamination [209–212]. Out of these, Wang et al., reviewed MOFs that are particularly useful for photocatalytic Cr(VI) reduction [209] and Wu et al., reviewed MOFs exclusively for photocatalytic degradation of

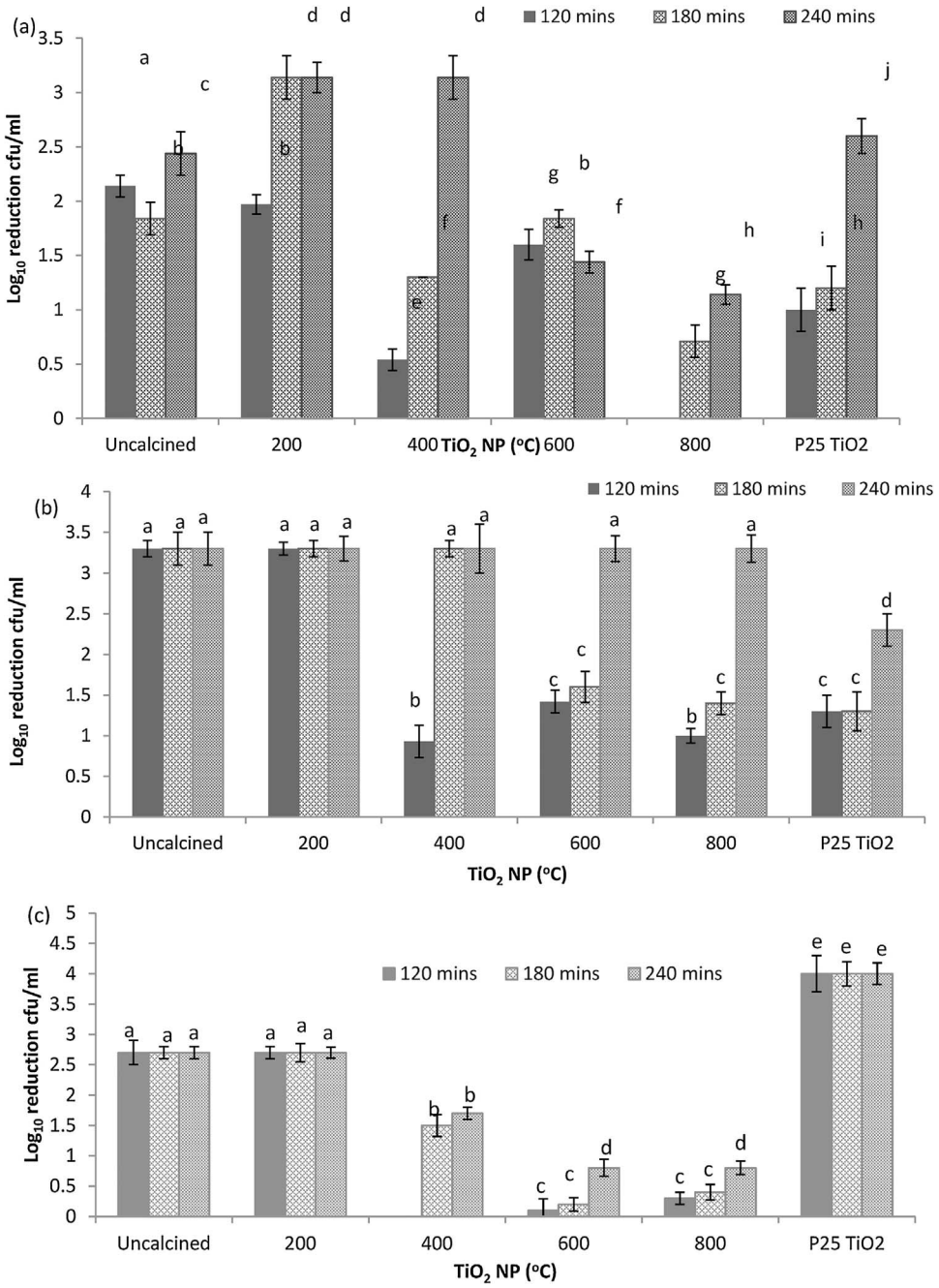

Fig. 22. Log_{10} cful/ml reduction in viable log phase bacterial numbers of (a) *S. typhimurium,* (b) *P. aeruginosa* and (c) *E. coli* (5 h cultures) with different TiO_2 nanotubes and control P25 TiO_2. a, b, c, d, e, f, g, h, i and j denotes significant difference at $p \leq 0.05$. [204] (Garvey et al., *Journal of Catalysis*, 631–639 (2016) 344). Copyright 2016, reprinted with permission from Elsevier.

organic dyes [210]. Herein, recent advances and out-of-ordinary strategies on the use of photocatalytic MOFs/composite of MOFs are presented. In addition, transformation of representative MOFs MIL-53(Cr, Al, and Fe) in aquatic environment and their toxicity are outlined.

A very interesting recent material in MOFs is – "MOF – Nanofiber Kebabs" [213]. This material was fabricated by deposition of TiO_2 on Polyamide-6 nanofibers *via* atomic layer deposition and subsequent growth of Zr-based MOFs such as UiO-66, UiO66-NH_2 and UiO67 on these TiO_2 deposited Polyamide-6 nanofibers (Figs. 23 and 24). Importantly, these MOF − Nanofiber Kebabs were excellent for detoxification of chemical warfare agents such as 4-nitrophenyl phosphate (Reactions in Fig. 25) and O-pinacolyl Methylphosphonofluoridate (known as GD) [213]. The study has a great social significance as it finds potential application in protective clothing for civilian and military personnel. Though the material does not require light for the detoxification, the strategy employed in the study offers scope for the development of photoreactive textile materials using MOFs.

Li et al., fabricated a TiO_2 encapsulated in Salicylaldehyde-NH_2-MIL-101(Cr) for photocatalytic degradation of MB [214]. TiO_2 was encapsulated by a unique environment created by introducing salicylaldehyde that provided a schiff base moiety in the porous NH_2-MIL-101(Cr). The resultant material was reusable and showed visible light promoted photocatalytic MB degradation. Moreover, the addition of H_2O_2 further enhanced the degradation efficiency [213]. Mixed metal organic frameworks (Mixed-MOFs) are another interesting class of MOFs that are constructed using more than one metal. Masoomi et al., synthesized Zn-based MOF (TMU-5), Cd-based MOF (TMU-7) and, zinc and cadmium mixed-MOFs (TMU-5(15% Cd) and TMU-5(30% Cd)) and

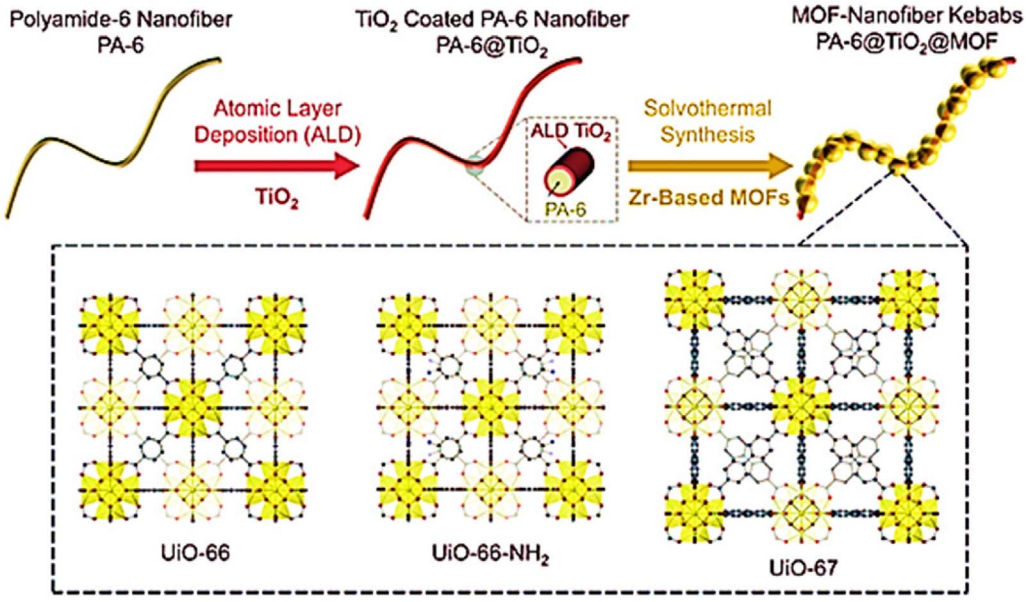

Fig. 23. Synthetic procedure for Zr- based nanofiber kebab structures on polyamide-6 nanofibers and the crystal structures of MOFs [213].

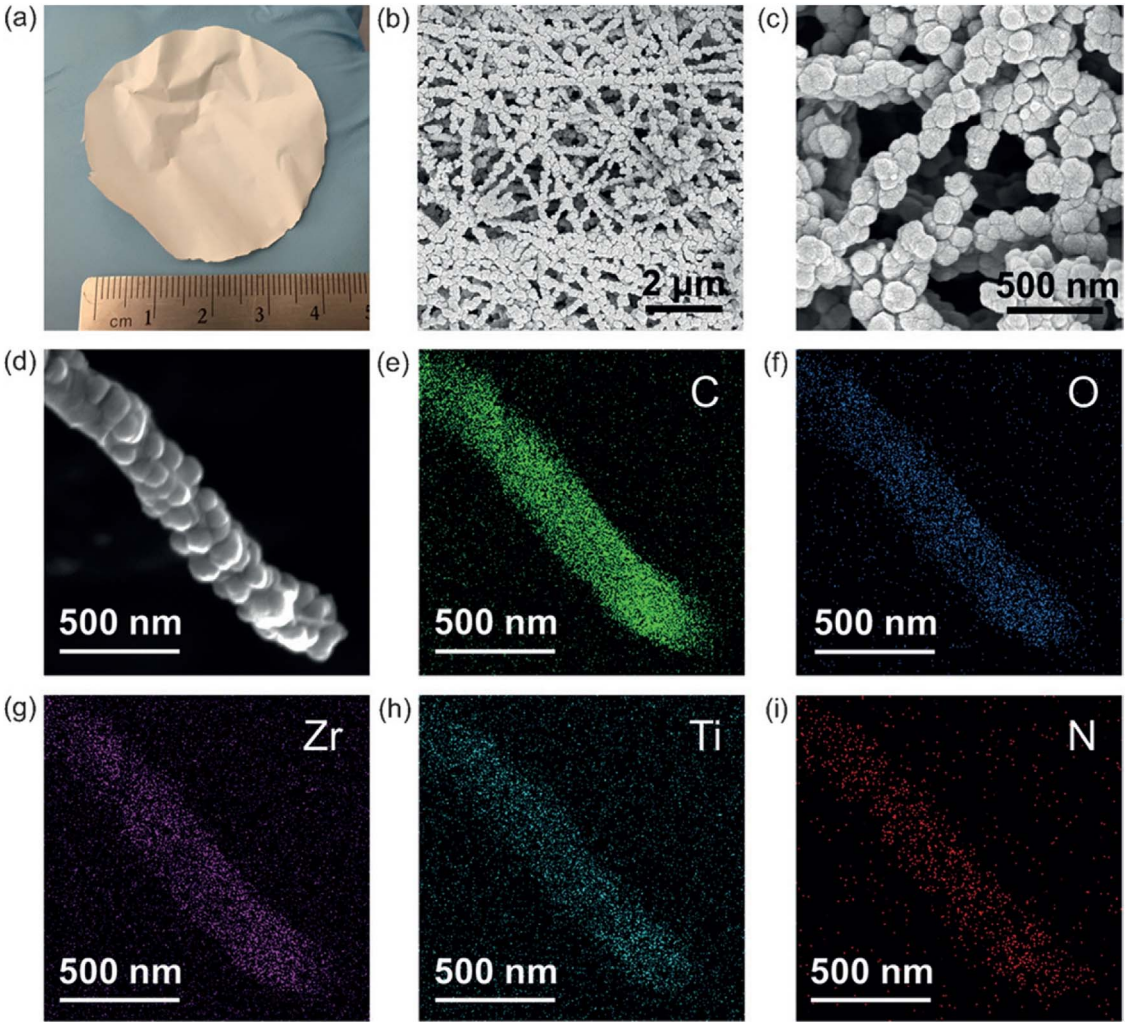

Fig. 24. a) Photo of a free-standing PA-6@TiO @UiO-66-NH_2 nanofiber mat [213] b–d) Scanning Electron Microscopy pictures of PA-6@TiO_2@UiO-66-NH_2. e–i) Energy dispersive X-ray mapping images of PA-6@TiO2@UiO-66-NH_2.

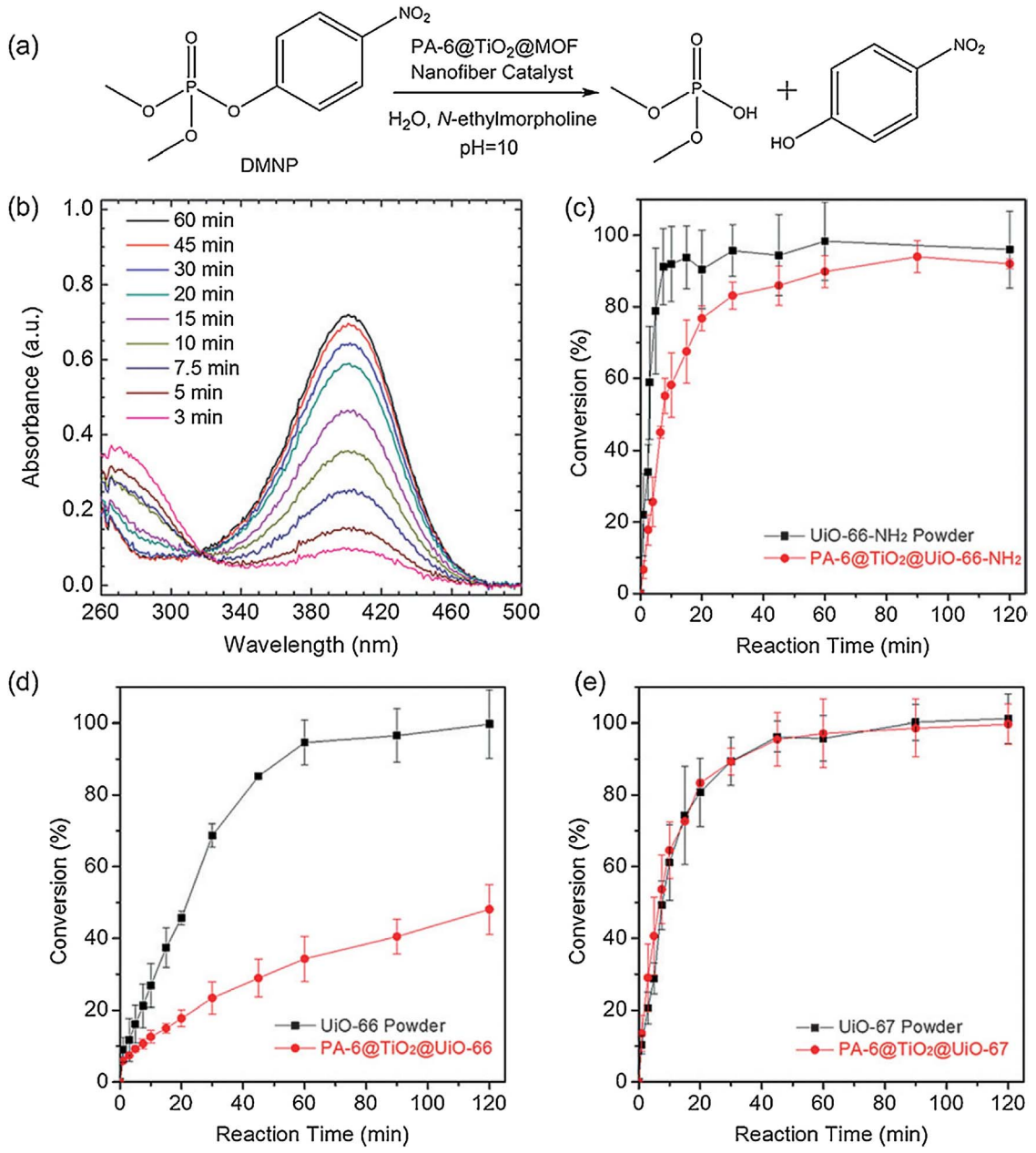

Fig. 25. a) Catalytic degradation of DMNP by MOF–nanofiber catalysts. b) UV/Vis spectra c–e) Conversion of DMNP to p-nitrophenoxide versus reaction time using powdered MOF and MOF–nanofiber catalysts [213].

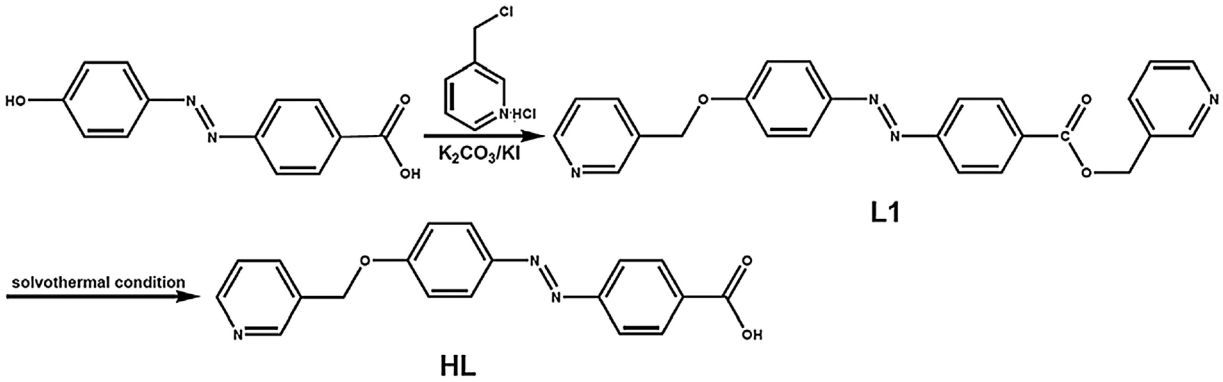

Fig. 26. Synthesis of (pyridin-3-yl)methyl 4-(2-(4-((pyridin3-yl)methoxy)phenyl)diazenyl)benzoate [216].

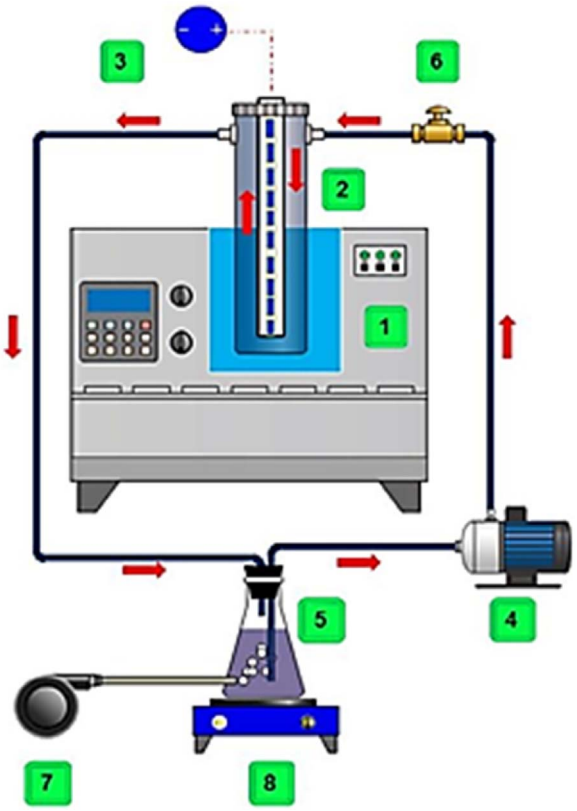

Fig. 27. Sonophotocatalytic reactor set-up, (1) ultrasonic bath, (2) reactor vessel, (3) LED source, (4) peristaltic pump, (5) reservoir, (6) sampling valve, (7) aeration pump, (8) magnet stirrer [217]. (Mosleh et al., *Ultrasonics Sonochemistry*, 387–397 (2016) 32). Copyright 2016, reprinted with permission from Elsevier.

evaluated their degradation efficiencies [215]. Results revealed that Zn-based MOF are better than Cd-based MOF. Importantly, zinc and cadmium mixed-MOFs showed remarkable photocatalytic degradation of phenol without addition of external oxidant such as H_2O_2 [215]. Notably, performance a MOF – TMU-5(30% Cd) was superior than P-25 TiO_2. As mentioned above, it's possible to tune the structures of MOFs by tuning the organic linkers. A new ligand, (pyridin-3-yl)methyl 4-(2-(4-((pyridin3-yl)methoxy)phenyl)diazenyl)benzoate (Fig. 26) was synthesized to fabricate five mixed metal Zn(II)/Cd(II) MOFs that showed photocatalytic MB degradation [216].

Different from the above studies, Mosleh et al., coupled sonocatalysis and a visible light active MOF – Ag_3PO_4/Bi_2S_3-HKUST-1 for simultaneous sonophotocatalytic degradation of organic dyes. Sonophotocatalytic degradation was performed using a continuous flow-loop reactor with blue light emitting LEDs as light source (Fig. 27) [217]. The continuous loop reactor increased the mass transfer rate by creating a turbulence caused by circulation of liquid. Moreover, the operational parameters were optimized by central composite design (CCD) combined with desirability function (DF). The effect of combining sonocatalysis with photocatalysis was evaluated using synergistic index. Results revealed that under optimized conditions, a significant synergy was observed in the simultaneous sonophotocatalytic degradation leading to excellent degradation of organic dyes [217]. The study indicates that coupling other AOPs with photocatalytic MOFs could be an effective strategy for water remediation.

The increasing development in MOF for various applications including water treatment calls for the fate of these materials in natural environment. The transformation of two representative MOFs MIL-53(Cr), MIL-53(Al) and MIL53(Fe) in aquatic environment, and their metal dependent reactive oxygen species generation was investigated [218]. The results revealed that hat the ROS production in MOF of type MIL-53 is dependent on the metal and displays different mechanism of ROS generation. Surprisingly, the toxicity of the MOF on the human liver cell lines (HepG2) followed the order MIL-53(Al) > MIL-53(Fe) > MIL-53(Cr) [218]. It is important to note that the toxicity of Cr(III) MIL-53 was significantly less than the presumably biocompatible Fe(III) MOF – Fe(III) MIL-53. The study indicates that further research is required to fully address the concerns regarding the fate of MOFs in aquatic environment when applied for water treatment processes (Table 1).

8. Conclusions

There has been an extensive amount of studies into photocatalysis since its first discovery. Titania still remains to be the photocatalyst of choice in many cases. This is due to a number of things which include low lost, nontoxicity and high oxidizing ability. In order to produce TiO_2 that is activated by both UV and visible light a number of methods have been deployed. These include forming heterojunctions (either with two of the titania phases or TiO_2 and another photocatalyst) and the use of dopants/chemical modifiers or additives in order to narrow the band gap. Both of these methods have been studied and been proven effective. Presently, chlorination or UVC disinfection is generally employed as a tertiary process in waste water treatment. TiO_2 photocatalysis is an effective alternate for these traditional processes and can be implemented for "treatment at source" such as in waste water treatment plants, ground water reclamation and storm water reuse. TiO_2 photocatalysis based AOPs can be developed further by integrating them with membrane filtration or fabricating photocatalytic TiO_2 membranes that are highly desirable in view of practical application in drinking water treatment.

There has been a growing interest in examining photocatalysts other than TiO_2, for example ZnO, CdS, ZnS, WO_3 and Fe_2O_3. Impact of dopants such as graphite-like C_3N_4, silver, chromium, aluminium, tin, cobalt and reduced graphene oxide on ZnO have been discussed [105,108–110,112–114,145,148–150,152–154]. Various novel doped visible light photocatalysts such as ZnS-CuS-CdS, carbon spheres/CdS, g-C_3N_4-Au-CdS, ZnS-WS_2-CdS, C_3N_4-CdS and Pd-Cr_2O_3-CdS have also been discussed. However, despite the growing interest into developing a visible light photocatalyst (by using TiO_2 or a novel material) there is still no standard reference material for visible light photoactivity to use as a comparison for novel work.

Photocatalysis has become a method that can effectively degrade and mineralize a variety of pesticide contaminants in the presence of TiO_2 and TiO_2 based nanocomposites. Endocrine disruptors are challenging pollutants as they transform to more toxic products or retain their endocrine disruption activity even after oxidative treatment. Though many studies on TiO_2 or TiO_2 based nanocomposites have been shown to degrade endocrine disruptors, the studies on the residual toxicity of the treated waste water is relatively low. The inactivation of bacteria has becoming an important research area in recent years for a number of applications, including in the environmental and in hospitals. TiO_2 has the ability to photocatalytically inactivate bacteria by damaging their cell walls and then oxidizing their internal components. A number of samples have been examined for this purpose. From these studies, it can be concluded that the inactivation of microbes is dependent on a number of properties of samples, *e.g.* the composition of the material, the phase of the sample, effective design of the reactors, the concentration and the irradiation source. Future studies in this direction have to be carried out along with the toxicological assays for evaluating the applicability of the process and also for further development. MOFs and its composites are receiving increasing attention due to their tunable photocatalytic properties. The studies on MOFs strongly supports that MOFs are effective alternates for metal oxide based photocatalysts for water decontamination.

Table 1
Brief summary of catalysts examined in this review.

Catalyst	Parameters	Application	Contaminate	Results	Ref.
ZnO	Heated at 600 °C. Compared to P25	Degradation of organic dye	Methylene orange	Rate of degradation with ZnO was 4 times faster than P25	[107]
ZnO- C_3N_4	ZnO doped with graphite-like C_3N_4	Degradation of organic dye	Methylene blue	The doped sample showed improvement of photoactivity by 5 times compared to ZnO	[108]
ZnO-graphene	ZnO_{1-x}/graphene	Degradation of organic dye	Methylene Blue	UV & Visible light activity was improved by 1.2 and 4.6 times respectively compared to ZnO	[105]
TiO_2	TiO_2 nanopowders (Aeroxide P25)	Degradation of contaminates of emerging concern (CECs)	1,4 Dioxane, n-nitrosodiummethylsmine (NDMA), tris-2-chloroethylphosphate (TCEP) Gemfibrozil, 17β estradiol	At optimum conditions (pH5 and TiO_2 1.5 g/L) 77% of 1,4 Dioxane, 92% of NDMA, 45% of TCEP, 95% of Gemfibrozil and 93% of 17β estradiol were degraded in 30 min	[147]
TiO_2	A sol containing TTIP, P25 & Polyethylene was dip-coated onto glass spheres	Degradation of CECs	Acetaminophen, antipyrine, atrazine, carbamazepine, diclofenac, flumequine, hydroxybiphenyl, ibuprofen, isoproturon, ketorolac, ofloxacin, progesterone, sulfamethoxazole and triclosan.	85% removal of the contaminates were removed by 120 min	[149]
TiO_2	TiO_2 deposits on stainless steel mesh, P25	Degradation of CECs	Warfarin, Trimethoprim, Metoprolol, Carbamazepine, Gemfibrozil, Terbutaline, Iopromide, 2,4 Dihydroxy-benzophenone, Perfluorooctanesulfonic acid, and Perfluorooctanoic acid	Performed better than P25. Toxicity assays shows a significant reduction in toxicity after treatment	[150]
TiO_2	Immobilized TiO_2 in the form of quartz fibre filters (QFT) & porous titanium sheets (PTT)	Degradation of CECs	Carbamazepine, Venlafaxine, Fluoxetine, Atenolol, Sulfamethoxazole, Ibuprofen, Atorvastatin, and Naproxen, Triclosan, Triclocarban and the metabolites of these contaminants including Carbamazepine-10,11-epoxide, Norfluoxetine, p-hydroxy atorvastatin, o-hydroxy atorvastatin	At optimum pH (4.5-5), QFT was negatively charged and PTT was positively charged. Cationic compounds were efficiently removed by QFT, while anionic compounds were remover by PTT.	[151]
TiO_2, N-TiO_2,	Nanocrystalline TiO_2, N- TiO_2, reduced Graphite oxide doped TiO_2	Degradation of Endocrine Disrupters and Pesticides	17β estradiol	After degradation to below its detection limit there was still residual estrogenic activity	[173]
TiO_2 & WO_3	TiO_2 & TiO_2-WO_3	Degradation of Endocrine Disrupters and Pesticides	17-α-ethinylestradiol	Both samples degraded the contaminate either by photocatalysis or electrochemical assisted photocatalysis. WO_3 prevented recombination resulting in increased activity	[176]
Pd- TiO_2	Pd doped TiO_2	Degradation of Endocrine Disrupters and Pesticides	4–Ntriophenol (or p – Nitophenol)	1.0 mol% was optiumum for the photocatalytic reduction	[178]
Fe_3O_4-SiO_2-TiO_2	TiO_2 doped with Fe_3O_4 and SiO_2-	Degradation of Endocrine Disrupters and Pesticides	Organophosphorus pesticides	More efficient in removal of pesticides such as acephate, omethoate and methyl parathion than P25. Acephate required 80 min of treatment, omethoate and methyl parathion need 50 min.	[191]
N-S-TiO_2	N and S doped TiO_2 @ 400 °C & 500 °C	Anti-microbial activity	*E. coli*	Varying the temp resulted in different doping species. *E. coli* was inactivated under UV and visible light, a result from the N-S doping	[200–203]
TiO_2 Heterojunctions	TiO_2 anatase: brookite (80:20)	Anti-microbial activity	*S. aureus*	Effective under visible light. Significant increase in photocatalysis and antibacterial properties	[50,52]
TiO_2 Nanotobes	TiO_2 nanotubes. Uncalcined, 200–800 °C. P25 for comparison	Anti-microbial activity	*S. typhimurium* *P. aeruginosa* *E. coli*	Controls showed no inactivation. As the temperature and% rutile increased the rate of inactivation.	[204]
TiO_2 on Polyminde-6 nanofibres	Deposit of TiO_2 on Polyminde-6 nanofibres *via* atomic layer deposition and subsequent growth of Zr-based MOFs, *e.g.* UiO-66, UiO67 & UiO-66NH_4	Metal Organic Frameworks (MOFs)	Nitrophenyl phosphate, O-pinacolyl Methylphosphonofluoridate	Has potential application in protective clothing. The strategy employed in the study offers scope for the development of photoreactive textile materials using MOFs.	[213]
TiO_2	TiO_2 encapsulated in Salicylaldehyde-NH_2-MIL-101(Cr)	MOFs/degradation of dyes	Methylene blue	Material was resilient and reusable. Showed visible light photodegradation. Adding H_2O_2 improved the efficiency of the photoactivity.	[213,214]

(continued on next page)

Table 1 *(continued)*

Catalyst	Parameters	Application	Contaminate	Results	Ref.
Cd And/or Zn	Zn-based MOF (TMU-5), Cd-based MOF (TMU-7) and, zinc and cadmium mixed-MOFs (TMU-5(15% Cd) and TMU-5(30% Cd))	MOFs	Phenol	Zn-based MOF was more active than the Cd-based MOF. The Zn-Cd mixed-MOF showed remarkable degradation without an external oxidant. TMU-5(30% Cd) showed more activity than P25.	[215]

References

[1] M. Pelaez, N.T. Nolan, S.C. Pillai, M.K. Seery, P. Falaras, A.G. Kontos, P.S. Dunlop, J.W. Hamilton, J.A. Byrne, K. O'shea, A review on the visible light active titanium dioxide photocatalysts for environmental applications, Appl. Catal. B: Environ. 125 (2012) 331–349.

[2] M.N. Chong, B. Jin, C.W. Chow, C. Saint, Recent developments in photocatalytic water treatment technology: a review, Water Res. 44 (2010) 2997–3027.

[3] R. George, N. Bahadur, N. Singh, R. Singh, A. Verma, A. Shukla, Environmentally benign TiO2 nanomaterials for removal of heavy metal ions with interfering ions present in tap water, Mater. Today:. Proc. 3 (2016) 162–166.

[4] M.I. Litter, Last advances on TiO 2-photocatalytic removal of chromium uranium and arsenic, Curr. Opin. Green Sustain. Chem. (2017) (in press, accepted manuscript).

[5] R. Molinari, C. Lavorato, P. Argurio, Recent progress of photocatalytic membrane reactors in water treatment and in synthesis of organic compounds. A review, Catal. Today 281 (2017) 144–164.

[6] A. Speltini, F. Maraschi, M. Sturini, V. Caratto, M. Ferretti, A. Profumo, Sorbents coupled to solar light tiO2-based photocatalysts for olive mill wastewater treatment, Int. J. Photoenergy 2016 (2016).

[7] M. Gmurek, M. Olak-Kucharczyk, S. Ledakowicz, Photochemical decomposition of endocrine disrupting compounds–a review, Chem. Eng. J. 310 (2017) 437–456.

[8] M. Hassan, Y. Zhao, B. Xie, Employing TiO 2 photocatalysis to deal with landfill leachate: current status and development, Chem. Eng. J. 285 (2016) 264–275.

[9] S. Kim, M. Kim, S.K. Lim, Y. Park, Titania-coated plastic optical fiber fabrics for remote photocatalytic degradation of aqueous pollutants, J. Environ. Chem. Eng. 5 (2017) 1899–1905.

[10] Y. Abdel-Maksoud, E. Imam, A. Ramadan, TiO2 solar photocatalytic reactor systems: selection of reactor design for scale-up and vommercialization—analytical review, Catalysts 6 (2016) 138.

[11] N.F. Moreira, J.M. Sousa, G. Macedo, A.R. Ribeiro, L. Barreiros, M. Pedrosa, J.L. Faria, M.F.R. Pereira, S. Castro-Silva, M.A. Segundo, Photocatalytic ozonation of urban wastewater and surface water using immobilized TiO 2 with LEDs: micropollutants, antibiotic resistance genes and estrogenic activity, Water Res. 94 (2016) 10–22.

[12] M. Borges, M. Sierra, E. Cuevas, R. García, P. Esparza, Photocatalysis with solar energy: sunlight-responsive photocatalyst based on TiO 2 loaded on a natural material for wastewater treatment, Sol. Energy 135 (2016) 527–535.

[13] S. Malato, M.I. Maldonado, P. Fernandez-Ibanez, I. Oller, I. Polo, R. Sanchez-Moreno, Decontamination and disinfection of water by solar photocatalysis: the pilot plants of the Plataforma Solar de Almeria, Mater. Sci. Semicond. Process. 42 (2016) 15–23.

[14] K.K. Philippe, R. Timmers, R. van Grieken, J. Marugan, Photocatalytic disinfection and removal of emerging pollutants from effluents of biological wastewater treatments, using a newly developed large-scale solar simulator, Ind. Eng. Chem. Res. 55 (2016) 2952–2958.

[15] M. Badia-Fabregat, I. Oller, S. Malato, Overview on Pilot-Scale Treatments and New and Innovative Technologies for Hospital Effluent, (2017).

[16] S. Challagulla, R. Nagarjuna, R. Ganesan, S. Roy, Acrylate-based polymerizable sol–gel synthesis of magnetically recoverable TiO2 supported Fe3O4 for Cr (VI) photoreduction in aerobic atmosphere, ACS Sustain. Chem. Eng. 4 (2016) 974–982.

[17] P.-Y. Wu, Y.-P. Jiang, Q.-Y. Zhang, Y. Jia, D.-Y. Peng, W. Xu, Comparative study on arsenate removal mechanism of MgO and MgO/TiO 2 composites: FTIR and XPS analysis, New J. Chem. 40 (2016) 2878–2885.

[18] D.A. Hanaor, C.C. Sorrell, Review of the anatase to rutile phase transformation, J. Mater. Sci. 46 (2011) 855–874.

[19] N. Shaham-Waldmann, Y. Paz, Away from TiO 2: a critical minireview on the developing of new photocatalysts for degradation of contaminants in water, Mater. Sci. Semicond. Process. 42 (2016) 72–80.

[20] K.K. Rao, G. Kumar, Polymorphic phase transition among the titania crystal structures in solution based approach: from precursor chemistry to nucleation process, Nanoscale 6 (2014) 11574–11632.

[21] A. Fujishima, K. Honda, Photolysis-decomposition of water at the surface of an irradiated semiconductor, Nature 238 (1972) 37–38.

[22] A.L. Linsebigler, G. Lu, J.T. Yates Jr., Photocatalysis on TiO2 surfaces: principles, mechanisms, and selected results, Chem. Rev. 95 (1995) 735–758.

[23] D.O. Scanlon, C.W. Dunnill, J. Buckeridge, S.A. Shevlin, A.J. Logsdail, S.M. Woodley, C.R.A. Catlow, M.J. Powell, R.G. Palgrave, I.P. Parkin, Band alignment of rutile and anatase TiO2, Nat. Mater. 12 (2013) 798–801.

[24] V. Etacheri, U. Geiger, Y. Gofer, G.A. Roberts, I.C. Stefan, R. Fasching, D. Aurbach, Exceptional electrochemical performance of Si-nanowires in 1, 3-dioxolane solutions: a surface chemical investigation, Langmuir 28 (2012) 6175–6184.

[25] D.M. Blake, Bibliography of Work on the Heterogeneous Photocatalytic Removal of Hazardous Compounds from Water and Air, National Renewable Energy Laboratory, 1994.

[26] S. Banerjee, S.C. Pillai, P. Falaras, K.E. O'Shea, J.A. Byrne, D.D. Dionysiou, New insights into the mechanism of visible light photocatalysis, J. Phys. Chem Lett. 5 (2014) 2543–2554.

[27] K. Hustert, R.G. Zepp, Photocatalytic degradation of selected azo dyes, Chemosphere 24 (1992) 335–342.

[28] R. Ojani, J.-B. Raoof, E. Zarei, Electrochemical monitoring of photoelectrocatalytic degradation of rhodamine B using TiO2 thin film modified graphite electrode, J. Solid State Electrochem. 16 (2012) 2143–2149.

[29] S. Banerjee, D.D. Dionysiou, S.C. Pillai, Self-cleaning applications of TiO 2 by

photo-induced hydrophilicity and photocatalysis, Appl. Catal. B: Environ. 176 (2015) 396–428.
[30] H. Gerischer, A. Heller, The role of oxygen in photooxidation of organic molecules on semiconductor particles, J. Phys. Chem. 95 (1991) 5261–5267.
[31] K. Vinodgopal, I. Bedja, S. Hotchandani, P.V. Kamat, A photocatalytic approach for the reductive decolorization of textile azo dyes in colloidal semiconductor suspensions, Langmuir 10 (1994) 1767–1771.
[32] K. Vinodgopal, P.V. Kamat, Photochemistry of textile azo dyes. Spectral characterization of excited state, reduced and oxidized forms of acid orange 7, J. Photochem. Photobiol. A: Chem. 83 (1994) 141–146.
[33] G. Shemer, Y. Paz, Interdigitated Electrophotocatalytic Cell for Water Purification, Int. J. Photoenergy, (2011).
[34] A. Okasha, F. Gomaa, H. Elhaes, M. Morsy, S. El-Khodary, A. Fakhry, M. Ibrahim, Spectroscopic analyses of the photocatalytic behavior of nano titanium dioxide, Spectrochim. Acta Part A 136 (2015) 504–509.
[35] S.C. Pillai, P. Periyat, R. George, D.E. McCormack, M.K. Seery, H. Hayden, J. Colreavy, D. Corr, S.J. Hinder, Synthesis of high-temperature stable anatase TiO2 photocatalyst, J. Phys. Chem. C 111 (2007) 1605–1611.
[36] N.T. Nolan, M.K. Seery, S.J. Hinder, L.F. Healy, S.C. Pillai, A systematic study of the effect of silver on the chelation of formic acid to a titanium precursor and the resulting effect on the anatase to rutile transformation of TiO2, J. Phys. Chem. C 114 (2010) 13026–13034.
[37] V. Etacheri, M.K. Seery, S.J. Hinder, S.C. Pillai, Highly visible light active tiO2- x N x heterojunction photocatalysts†, Chem. Mater. 22 (2010) 3843–3853.
[38] M.K. Seery, R. George, P. Floris, S.C. Pillai, Silver doped titanium dioxide nanomaterials for enhanced visible light photocatalysis, J. Photochem. Photobiol. A: Chem. 189 (2007) 258–263.
[39] C. Byrne, R. Fagan, S. Hinder, D.E. McCormack, S.C. Pillai, New approach of modifying the anatase to rutile transition temperature in TiO 2 photocatalysts, RSC Adv. 6 (2016) 95232–95238.
[40] N.S. Leyland, J. Podporska-Carroll, J. Browne, S.J. Hinder, B. Quilty, S.C. Pillai, Highly efficient F, Cu doped TiO2 anti-bacterial visible light active photocatalytic coatings to combat hospital-acquired infections, Sci. Rep. 6 (2016).
[41] E.F. Heald, C.W. Weiss, Kinetics and mechanism of anatase/rutile transformation, as catalyzed by ferric oxide and reducing conditions, Am. Mineral. 57 (1972) 10- & .
[42] Y. Hu, H.L. Tsai, C.L. Huang, Effect of brookite phase on the anatase–rutile transition in titania nanoparticles, J. Eur. Ceram. Soc. 23 (2003) 691–696.
[43] O. Carp, C.L. Huisman, A. Reller, Photoinduced reactivity of titanium dioxide, Prog. Solid State Chem. 32 (2004) 33–177.
[44] R.F. de Farias, C.C. Silva, T.A. Restivo, Thermal study of the anatase-rutile structural transitions in sol-gel synthesized titanium dioxide powders, J. Serb. Chem. Soc. 70 (2005) 675–679.
[45] P. Periyat, S.C. Pillai, D.E. McCormack, J. Colreavy, S.J. Hinder, Improved high-temperature stability and sun-light-driven photocatalytic activity of sulfur-doped anatase TiO2, J. Phys. Chem. C 112 (2008) 7644–7652.
[46] N.T. Nolan, M.K. Seery, S.C. Pillai, Spectroscopic investigation of the anatase-to-rutile transformation of sol- gel-synthesized TiO2 photocatalysts, J. Phys. Chem. C 113 (2009) 16151–16157.
[47] C. Byun, J.W. Jang, I.T. Kim, K.S. Hong, B.W. Lee, Anatase-to-rutile transition of titania thin films prepared by MOCVD, Mater. Res. Bull. 32 (1997) 431–440.
[48] A. Markowska-Szczupak, K. Ulfig, A. Morawski, The application of titanium dioxide for deactivation of bioparticulates: an overview, Catal. Today 169 (2011) 249–257.
[49] V. Etacheri, M.K. Seery, S.J. Hinder, S.C. Pillai, Oxygen rich titania: a dopant free, high temperature stable, and visible-light active anatase photocatalyst, Adv. Funct. Mater. 21 (2011) 3744–3752.
[50] R. Fagan, D.E. McCormack, D.D. Dionysiou, S.C. Pillai, A review of solar and visible light active TiO 2 photocatalysis for treating bacteria, cyanotoxins and contaminants of emerging concern, Mater. Sci. Semicond. Process. 42 (2015) 2–14.
[51] M.B. Fisher, D.A. Keane, P. Fernandez-Ibanez, J. Colreavy, S.J. Hinder, K.G. McGuigan, S.C. Pillai, Nitrogen and copper doped solar light active TiO 2 photocatalysts for water decontamination, Appl. Catal. B: Environ. 130 (2013) 8–13.
[52] V. Etacheri, G. Michlits, M.K. Seery, S.J. Hinder, S.C. Pillai, A highly efficient TiO2–x C x nano-heterojunction photocatalyst for visible light induced antibacterial applications, ACS Appl. Mater. Interfaces 5 (2013) 1663–1672.
[53] J. Hamilton, T. Byrne, P. Dunlop, D.D. Dionysiou, M. Pelaez, K.E. O'Shea, D. Synnott, S.C. Pillai, Evaluating the mechanism of visible light activity for N, F-TiO2 using photoelectrochemistry, J. Phys. Chem. C 118 (2014) 12206–12215.
[54] T. Ohno, K. Sarukawa, M. Matsumura, Photocatalytic activities of pure rutile particles isolated from TiO2 powder by dissolving the anatase component in HF solution, J. Phys. Chem. B 105 (2001) 2417–2420.
[55] D.S. Muggli, L. Ding, Photocatalytic performance of sulfated TiO 2 and Degussa P-25 TiO 2 during oxidation of organics, Appl. Catal. B: Environ. 32 (2001) 181–194.
[56] Z. Zhang, C.-C. Wang, R. Zakaria, J.Y. Ying, Role of particle size in nanocrystalline TiO2-based photocatalysts, J. Phys. Chem. B 102 (1998) 10871–10878.
[57] R.I. Bickley, T. Gonzalez-Carreno, J.S. Lees, L. Palmisano, R.J. Tilley, A structural investigation of titanium dioxide photocatalysts, J. Solid State Chem. 92 (1991) 178–190.
[58] Q. Zhang, L. Gao, J. Guo, Effects of calcination on the photocatalytic properties of nanosized TiO 2 powders prepared by TiCl 4 hydrolysis, Appl. Catal. B: Environ. 26 (2000) 207–215.
[59] R. Bacsa, J. Kiwi, Effect of rutile phase on the photocatalytic properties of nanocrystalline titania during the degradation of p-coumaric acid, Appl. Catal. B: Environ. 16 (1998) 19–29.
[60] T. Ohno, K. Tokieda, S. Higashida, M. Matsumura, Synergism between rutile and anatase TiO 2 particles in photocatalytic oxidation of naphthalene, Appl. Catal. A: Gen. 244 (2003) 383–391.
[61] M. Batzill, E.H. Morales, U. Diebold, Influence of nitrogen doping on the defect formation and surface properties of TiO 2 rutile and anatase, Phys. Rev. Lett. 96 (2006) 026103.
[62] D.C. Hurum, A.G. Agrios, K.A. Gray, T. Rajh, M.C. Thurnauer, Explaining the enhanced photocatalytic activity of Degussa P25 mixed-phase TiO2 using EPR, J. Phys. Chem. B 107 (2003) 4545–4549.
[63] V. Loddo, G. Marci, L. Palmisano, A. Sclafani, Preparation and characterization of Al 2 O 3 supported TiO 2 catalysts employed for 4-nitrophenol photodegradation in aqueous medium, Mater. Chem. Phys. 53 (1998) 217–224.
[64] A. Sclafani, J. Herrmann, Comparison of the photoelectronic and photocatalytic activities of various anatase and rutile forms of titania in pure liquid organic phases and in aqueous solutions, J. Phys. Chem. 100 (1996) 13655–13661.
[65] Y. Bessekhouad, D. Robert, J. Weber, Preparation of TiO2 nanoparticles by sol-gel route, Int. J. Photoenergy 5 (2003) 153–158.
[66] A. Mills, N. Elliott, G. Hill, D. Fallis, J.R. Durrant, R.L. Willis, Preparation and characterisation of novel thick sol–gel titania film photocatalysts, Photochem. Photobiol. Sci. 2 (2003) 591–596.
[67] H. Zhang, J.F. Banfield, Phase transformation of nanocrystalline anatase-to-rutile via combined interface and surface nucleation, J. Mater. Res. 15 (2000) 437–448.
[68] A. Navrotsky, O. Kleppa, Enthalpy of the anatase-rutile transformation, J. Am. Ceram. Soc. 50 (1967) 626-626.
[69] Z. Shi, L. Yan, L. Jin, X. Lu, G. Zhao, The phase transformation behaviors of Sn 2+-doped Titania gels, J. Non-Cryst. Solids 353 (2007) 2171–2178.
[70] H. Shin, H.S. Jung, K.S. Hong, J.-K. Lee, Crystal phase evolution of TiO 2 nanoparticles with reaction time in acidic solutions studied via freeze-drying method, J. Solid State Chem. 178 (2005) 15–21.
[71] G.H. Lee, J.M. Zuo, Growth and phase transformation of nanometer-sized titanium oxide powders produced by the precipitation method, J. Am. Ceram. Soc. 87 (2004) 473–479.
[72] C. Suresh, V. Biju, P. Mukundan, K. Warrier, Anatase to rutile transformation in sol-gel titania by modification of precursor, Polyhedron 17 (1998) 3131–3135.
[73] L. Hu, T. Yoko, H. Kozuka, S. Sakka, Effects of solvent on properties of sol—gel-derived TiO2 coating films, Thin Solid Films 219 (1992) 18–23.
[74] V. Etacheri, C. Di Valentin, J. Schneider, D. Bahnemann, S.C. Pillai, Visible-light activation of TiO2 photocatalysts: advances in theory and experiments, J. Photochem. Photobio. C: Photo Chem. Rev. 25 (2015) 1–29.
[75] H. Irie, Y. Watanabe, K. Hashimoto, Carbon-doped anatase TiO2 powders as a visible-light sensitive photocatalyst, Chem. Lett. 32 (2003) 772–773.
[76] S. Sakthivel, H. Kisch, Daylight photocatalysis by carbon-modified titanium dioxide, Angew. Chem. Int. Ed. 42 (2003) 4908–4911.
[77] C. Byrne, R. Fagan, S. Hinder, D.E. McCormack, S.C. Pillai, New approach of modifying the anatase to rutile transition temperature in TiO2 photocatalysts, RSC Adv. 6 (2016) 95232–95238.
[78] A. Fujishima, X. Zhang, Titanium dioxide photocatalysis: present situation and future approaches, Comptes Rendus Chimie 9 (2006) 750–760.
[79] F.E. Oropeza, J. Harmer, R. Egdell, R.G. Palgrave, A critical evaluation of the mode of incorporation of nitrogen in doped anatase photocatalysts, Phys. Chem. Chem. Phys. 12 (2010) 960–969.
[80] H. Choi, M.G. Antoniou, M. Pelaez, A.A. De la Cruz, J.A. Shoemaker, D.D. Dionysiou, Mesoporous nitrogen-doped TiO2 for the photocatalytic destruction of the cyanobacterial toxin microcystin-LR under visible light irradiation, Environ. Sci. Technol. 41 (2007) 7530–7535.
[81] X. Fang, Z. Zhang, Q. Chen, H. Ji, X. Gao, Dependence of nitrogen doping on TiO 2 precursor annealed under NH 3 flow, J. Solid State Chem. 180 (2007) 1325–1332.
[82] R. Asahi, T. Morikawa, T. Ohwaki, K. Aoki, Y. Taga, Visible-light photocatalysis in nitrogen-doped titanium oxides, Science 293 (2001) 269–271.
[83] H.M. Yadav, S.V. Otari, V.B. Koli, S.S. Mali, C.K. Hong, S.H. Pawar, S.D. Delekar, Preparation and characterization of copper-doped anatase TiO 2 nanoparticles with visible light photocatalytic antibacterial activity, J. Photochem. Photobiol. A: Chem. 280 (2014) 32–38.
[84] W. Ho, C.Y. Jimmy, S. Lee, Low-temperature hydrothermal synthesis of S-doped TiO 2 with visible light photocatalytic activity, J. Solid State Chem. 179 (2006) 1171–1176.
[85] S.C. Padmanabhan, S.C. Pillai, J. Colreavy, S. Balakrishnan, D.E. McCormack, T.S. Perova, Y. Gun'ko, S.J. Hinder, J.M. Kelly, A simple sol-gel processing for the development of high-temperature stable photoactive anatase titania, Chem. Mater. 19 (2007) 4474–4481.
[86] A. Czoska, S. Livraghi, M. Chiesa, E. Giamello, S. Agnoli, G. Granozzi, E. Finazzi, C.D. Valentin, G. Pacchioni, The nature of defects in fluorine-doped TiO2, J. Phys. Chem. C 112 (2008) 8951–8956.
[87] D. Li, H. Haneda, N.K. Labhsetwar, S. Hishita, N. Ohashi, Visible-light-driven photocatalysis on fluorine-doped TiO 2 powders by the creation of surface oxygen vacancies, Chem. Phys. Lett. 401 (2005) 579–584.
[88] R. Janes, L. Knightley, C. Harding, Structural and spectroscopic studies of iron (III) doped titania powders prepared by sol-gel synthesis and hydrothermal processing, Dyes Pigm. 62 (2004) 199–212.
[89] L. Kőrösi, S. Papp, J. Ménesi, E. Illés, V. Zöllmer, A. Richardt, I. Dékány, Photocatalytic activity of silver-modified titanium dioxide at solid–liquid and solid–gas interfaces, Coll. Surf. A 319 (2008) 136–142.
[90] S. Karvinen, The effects of trace elements on the crystal properties of TiO 2, Solid State Sci. 5 (2003) 811–819.
[91] K.C. Heo, C.I. Ok, J.W. Kim, B.K. Moon, The effects of manganese ions and their

magnetic properties on the anatase-rutile phase transition of nanocrystalline TiO2: Mn prepared by using the solvothermal method, J. Korean Phys. Soc. 47 (2005) 861–865.
[92] R. Arroyo, G. Cordoba, J. Padilla, V. Lara, Influence of manganese ions on the anatase–rutile phase transition of TiO 2 prepared by the sol–gel process, Mater. Lett. 54 (2002) 397–402.
[93] M. Seery, Metal Oxide Photocatalysis, The Photochemistry Portal, (2009).
[94] T.P. Portal, Metal Oxide Photocatalysis, (2009).
[95] V. Etacheri, M.K. Seery, S.J. Hinder, S.C. Pillai, Nanostructured ti1-x S x O2-y N y heterojunctions for efficient visible-light-induced photocatalysis, Inorg. Chem. 51 (2012) 7164–7173.
[96] W. Koppenol, J.F. Liebman, The oxidizing nature of the hydroxyl radical. A comparison with the ferryl ion (FeO2 +), J. Phys. Chem. 88 (1984) 99–101.
[97] N. Serpone, E. Pelizzetti, Photocatalysis: Fundamentals and Applications, Wiley-Interscience, 1989.
[98] W.-J. Chun, A. Ishikawa, H. Fujisawa, T. Takata, J.N. Kondo, M. Hara, M. Kawai, Y. Matsumoto, K. Domen, Conduction and valence band positions of Ta2O5, TaON, and Ta3N5 by UPS and electrochemical methods, J. Phys. Chem. B 107 (2003) 1798–1803.
[99] L. Wang, P. Wang, B. Huang, X. Ma, G. Wang, Y. Dai, X. Zhang, X. Qin, Synthesis of Mn-doped ZnS microspheres with enhanced visible light photocatalytic activity, Appl. Surf. Sci. 391 (2017) 557–564.
[100] C.-J. Chang, K.-W. Chu, M.-H. Hsu, C.-Y. Chen, Ni-doped ZnS decorated graphene composites with enhanced photocatalytic hydrogen-production performance, Int. J. Hydrogen Energy 40 (2015) 14498–14506.
[101] J. Vinoth Kumar, K. Saravanakumar, P. Senthil Kumar, V. Muthuraj, Visible light photocatalytic activity of rhombus like α-Fe2O3 for degradation of organic contaminants, Energy Environ. Focus 5 (2016) 222–228.
[102] L.Y. Huang, R.X. Zhang, X.J. Sun, X.N. Cheng, Synthesis and Characterization of g-C3N4/α-Fe2O3 Composites with Enhanced Photocatalytic Activity, Key Engineering Materials, Trans Tech Publ, 2014, pp. 225–228.
[103] M. Mahadik, S. Shinde, V. Mohite, S. Kumbhar, K. Rajpure, A. Moholkar, J. Kim, C. Bhosale, Photoelectrocatalytic oxidation of Rhodamine B with sprayed α-Fe2O3 photocatalyst, Mater. Express 3 (2013) 247–255.
[104] S. Pasternak, Y. Paz, On the similarity and dissimilarity between photocatalytic water splitting and photocatalytic degradation of pollutants, ChemPhysChem 14 (2013) 2059–2070.
[105] X. Bai, L. Wang, R. Zong, Y. Lv, Y. Sun, Y. Zhu, Performance enhancement of ZnO photocatalyst via synergic effect of surface oxygen defect and graphene hybridization, Langmuir 29 (2013) 3097–3105.
[106] J.-H. Sun, S.-Y. Dong, Y.-K. Wang, S.-P. Sun, Preparation and photocatalytic property of a novel dumbbell-shaped ZnO microcrystal photocatalyst, J. Hazard. Mater. 172 (2009) 1520–1526.
[107] C. Tian, Q. Zhang, A. Wu, M. Jiang, Z. Liang, B. Jiang, H. Fu, Cost-effective large-scale synthesis of ZnO photocatalyst with excellent performance for dye photodegradation, Chem. Commun. 48 (2012) 2858–2860.
[108] Y. Wang, R. Shi, J. Lin, Y. Zhu, Enhancement of photocurrent and photocatalytic activity of ZnO hybridized with graphite-like C 3 N 4, Energy Environ. Sci. 4 (2011) 2922–2929.
[109] C. Wu, L. Shen, Y.-C. Zhang, Q. Huang, Solvothermal synthesis of Cr-doped ZnO nanowires with visible light-driven photocatalytic activity, Mater. Lett. 65 (2011) 1794–1796.
[110] W. Xie, Y. Li, W. Sun, J. Huang, H. Xie, X. Zhao, Surface modification of ZnO with Ag improves its photocatalytic efficiency and photostability, J. Photochem. Photobiol. A: Chem. 216 (2010) 149–155.
[111] L.-Y. Yang, S.-Y. Dong, J.-H. Sun, J.-L. Feng, Q.-H. Wu, S.-P. Sun, Microwave-assisted preparation, characterization and photocatalytic properties of a dumbbell-shaped ZnO photocatalyst, J. Hazard. Mater. 179 (2010) 438–443.
[112] M. Ahmad, E. Ahmed, Y. Zhang, N. Khalid, J. Xu, M. Ullah, Z. Hong, Preparation of highly efficient Al-doped ZnO photocatalyst by combustion synthesis, Curr. Appl. Phys. 13 (2013) 697–704.
[113] J.-H. Sun, S.-Y. Dong, J.-L. Feng, X.-J. Yin, X.-C. Zhao, Enhanced sunlight photocatalytic performance of Sn-doped ZnO for methylene blue degradation, J. Mol. Catal. A: Chem. 335 (2011) 145–150.
[114] C. Xu, L. Cao, G. Su, W. Liu, X. Qu, Y. Yu, Preparation, characterization and photocatalytic activity of Co-doped ZnO powders, J. Alloys Compd. 497 (2010) 373–376.
[115] G. Chen, F. Li, Y. Fan, Y. Luo, D. Li, Q. Meng, A novel noble metal-free ZnS–WS 2/CdS composite photocatalyst for H 2 evolution under visible light irradiation, Catal. Commun. 40 (2013) 51–54.
[116] J. Fu, B. Chang, Y. Tian, F. Xi, X. Dong, Novel C 3 N 4–CdS composite photocatalysts with organic–inorganic heterojunctions: in situ synthesis, exceptional activity, high stability and photocatalytic mechanism, J. Mater. Chem. A 1 (2013) 3083–3090.
[117] E. Hong, D. Kim, J.H. Kim, Heterostructured metal sulfide (ZnS–CuS–CdS) photocatalyst for high electron utilization in hydrogen production from solar water splitting, J. Ind. Eng. Chem. 20 (2014) 3869–3874.
[118] Q. Li, B. Guo, J. Yu, J. Ran, B. Zhang, H. Yan, J.R. Gong, Highly efficient visible-light-driven photocatalytic hydrogen production of CdS-cluster-decorated graphene nanosheets, J. Am. Chem. Soc. 133 (2011) 10878–10884.
[119] X. Li, J. Chen, H. Li, J. Li, Y. Xu, Y. Liu, J. Zhou, Photoreduction of CO2 to methanol over Bi2S3/CdS photocatalyst under visible light irradiation, J. Nat. Gas Chem. 20 (2011) 413–417.
[120] W. Li, C. Feng, S. Dai, J. Yue, F. Hua, H. Hou, Fabrication of sulfur-doped gC 3 N 4/Au/CdS Z-scheme photocatalyst to improve the photocatalytic performance under visible light, Appl. Catal. B: Environ. 168 (2015) 465–471.
[121] J.-C. Wu, J. Zheng, P. Wu, R. Xu, Study of native defects and transition-metal (Mn, Fe, Co, and Ni) doping in a zinc-blende CdS photocatalyst by DFT and hybrid DFT calculations, J. Phys. Chem. C 115 (2011) 5675–5682.
[122] H. Yan, J. Yang, G. Ma, G. Wu, X. Zong, Z. Lei, J. Shi, C. Li, Visible-light-driven hydrogen production with extremely high quantum efficiency on Pt–PdS/CdS photocatalyst, J. Catal. 266 (2009) 165–168.
[123] W. Yao, C. Huang, N. Muradov, T. Ali, A novel Pd–Cr 2 O 3/CdS photocatalyst for solar hydrogen production using a regenerable sacrificial donor, Int. J. Hydrogen Energy 36 (2011) 4710–4715.
[124] W. Zhang, Y. Wang, Z. Wang, Z. Zhong, R. Xu, Highly efficient and noble metal-free NiS/CdS photocatalysts for H 2 evolution from lactic acid sacrificial solution under visible light, Chem. Commun. 46 (2010) 7631–7633.
[125] N. Zhang, Y. Zhang, X. Pan, X. Fu, S. Liu, Y.-J. Xu, Assembly of CdS nanoparticles on the two-dimensional graphene scaffold as visible-light-driven photocatalyst for selective organic transformation under ambient conditions, J. Phys. Chem. C 115 (2011) 23501–23511.
[126] Q. Cai, Z. Hu, Q. Zhang, B. Li, Z. Shen, Fullerene (C 60)/CdS nanocomposite with enhanced photocatalytic activity and stability, Appl. Surf. Sci. 403 (2017) 151–158.
[127] Q. Wang, J. Lian, Q. Ma, S. Zhang, J. He, J. Zhong, J. Li, H. Huang, B. Su, Preparation of carbon spheres supported CdS photocatalyst for enhancement its photocatalytic H 2 evolution, Catal. Today 281 (2017) 662–668.
[128] Z. Yue, A. Liu, C. Zhang, J. Huang, M. Zhu, Y. Du, P. Yang, Noble-metal-free hetero-structural CdS/Nb 2 O 5/N-doped-graphene ternary photocatalytic system as visible-light-driven photocatalyst for hydrogen evolution, Appl. Catal. B: Environ. 201 (2017) 202–210.
[129] X. Ning, S. Meng, X. Fu, X. Ye, S. Chen, Efficient utilization of photogenerated electrons and holes for photocatalytic selective organic syntheses in one reaction system using a narrow band gap CdS photocatalyst, Green Chem. 18 (2016) 3628–3639.
[130] P.S. Yoo, D.A. Reddy, Y. Jia, S.E. Bae, S. Huh, C. Liu, Magnetic core-shell ZnFe 2 O 4/ZnS nanocomposites for photocatalytic application under visible light, J. Colloid Interface Sci. 486 (2017) 136–143.
[131] L. Kong, Z. Li, S. Huang, J. Jia, L. Li, Boosting photocatalytic performance and stability of CuInS 2/ZnS-TiO 2 heterostructures via sol-gel processed integrate amorphous titania gel, Appl. Catal. B: Environ. 204 (2017) 403–410.
[132] M. Madkour, F. Al Sagheer, Au/ZnS and Ag/ZnS nanoheterostructures as re-generated nanophotocatalysts for photocatalytic degradation of organic dyes, Opt. Mater. Express 7 (2017) 158–169.
[133] D. Samanta, T.I. Chanu, S. Chatterjee, Citrus limetta juice as capping agent in hydrothermal synthesis of ZnS nanosphere for photocatalytic activity, Mater. Res. Bull. 88 (2017) 85–90.
[134] G.-J. Lee, S. Anandan, S.J. Masten, J.J. Wu, Photocatalytic hydrogen evolution from water splitting using Cu doped ZnS microspheres under visible light irradiation, Renewable Energy 89 (2016) 18–26.
[135] C.-J. Chang, K.-W. Chu, ZnS/polyaniline composites with improved dispersing stability and high photocatalytic hydrogen production activity, Int. J. Hydrogen Energy 41 (2016) 21764–21773.
[136] C.-J. Chang, K.-L. Huang, J.-K. Chen, K.-W. Chu, M.-H. Hsu, Improved photocatalytic hydrogen production of ZnO/ZnS based photocatalysts by Ce doping, J. Taiwan Inst. Chem. Eng. 55 (2015) 82–89.
[137] P. Suyana, S.N. Kumar, B.D. Kumar, B.N. Nair, S.C. Pillai, A.P. Mohamed, K. Warrier, U. Hareesh, Antifungal properties of nanosized ZnS particles synthesised by sonochemical precipitation, RSC Adv. 4 (2014) 8439–8445.
[138] A. Eyasu, O. Yadav, R. Bachheti, Photocatalytic degradation of methyl orange dye using Cr-doped ZnS nanoparticles under visible radiation, Int. J. Chem. Technol. Res. 5 (2013) 1452–1461.
[139] B. Petrie, R. Barden, B. Kasprzyk-Hordern, A review on emerging contaminants in wastewaters and the environment: current knowledge, understudied areas and recommendations for future monitoring, Water Res. 72 (2015) 3–27.
[140] A. Cesaro, V. Belgiorno, Removal of endocrine disruptors from urban wastewater by advanced oxidation processes (AOPs): a review, Open Biotechnol. J. 10 (2016).
[141] E. Kumar, W.V. Holt, Impacts of Endocrine Disrupting Chemicals on Reproduction in Wildlife, Reproductive Sciences in Animal Conservation, Springer, 2014, pp. 55–70.
[142] E. Marti, E. Variatza, J.L. Balcazar, The role of aquatic ecosystems as reservoirs of antibiotic resistance, Trends Microbiol. 22 (2014) 36–41.
[143] S.R. Hughes, P. Kay, L.E. Brown, Global synthesis and critical evaluation of pharmaceutical data sets collected from river systems, Environ. Sci. Technol. 47 (2012) 661–677.
[144] N. Nakada, S. Hanamoto, M.D. Jürgens, A.C. Johnson, M.J. Bowes, H. Tanaka, Assessing the population equivalent and performance of wastewater treatment through the ratios of pharmaceuticals and personal care products present in a river basin: application to the River Thames basin, UK, Sci. Total Environ. 575 (2017) 1100–1108.
[145] P. Kay, S.R. Hughes, J.R. Ault, A.E. Ashcroft, L.E. Brown, Widespread routine occurrence of pharmaceuticals in sewage effluent, combined sewer overflows and receiving waters, Environ. Pollut. 220 (2017) 1447–1455.
[146] S. Gaw, K.V. Thomas, T.H. Hutchinson, Sources, impacts and trends of pharmaceuticals in the marine and coastal environment, Phil. Trans. R. Soc. B 369 (2014) 20130572.
[147] J.R. Alvarez-Corena, J.A. Bergendahl, F.L. Hart, Advanced oxidation of five contaminants in water by UV/TiO 2: reaction kinetics and byproducts identification, J. Environ. Manage. 181 (2016) 544–551.
[148] E. Pino, M.V. Encinas, Photocatalytic degradation of chlorophenols on TiO2-325 mesh and TiO2-P25. An extended kinetic study of photodegradation under

competitive conditions, J. Photochem. Photobiol. A: Chem. 242 (2012) 20–27.
[149] N. Miranda-García, S. Suárez, B. Sánchez, J.M. Coronado, S. Malato, M.I. Maldonado, Photocatalytic degradation of emerging contaminants in municipal wastewater treatment plant effluents using immobilized TiO2 in a solar pilot plant, Appl. Catal. B: Environ. 103 (2011) 294–301.
[150] S. Murgolo, V. Yargeau, R. Gerbasi, F. Visentin, N. El Habra, G. Ricco, I. Lacchetti, M. Carere, M.L. Curri, G. Mascolo, A new supported TiO 2 film deposited on stainless steel for the photocatalytic degradation of contaminants of emerging concern, Chem. Eng. J. 318 (2016) 103–111.
[151] M.J. Arlos, M.M. Hatat-Fraile, R. Liang, L.M. Bragg, N.Y. Zhou, S.A. Andrews, M.R. Servos, Photocatalytic decomposition of organic micropollutants using immobilized TiO 2 having different isoelectric points, Water Res. 101 (2016) 351–361.
[152] R. Liang, A. Hu, W. Li, Y.N. Zhou, Enhanced degradation of persistent pharmaceuticals found in wastewater treatment effluents using TiO2 nanobelt photocatalysts, J. Nanopart. Res. 15 (2013).
[153] F. Loosli, L. Vitorazi, J.-F. Berret, S. Stoll, Towards a better understanding on agglomeration mechanisms and thermodynamic properties of TiO 2 nanoparticles interacting with natural organic matter, Water Res. 80 (2015) 139–148.
[154] F. Loosli, P. Le Coustumer, S. Stoll, Effect of natural organic matter on the disagglomeration of manufactured TiO 2 nanoparticles, Environ. Sci. Nano 1 (2014) 154–160.
[155] H. Peng, Y. Chen, L. Mao, X. Zhang, Significant changes in the photo-reactivity of TiO 2 in the presence of a capped natural dissolved organic matter layer, Water Res. 110 (2017) 233–240.
[156] S.L. Gora, S.A. Andrews, Adsorption of natural organic matter and disinfection byproduct precursors from surface water on TiO 2 nanoparticles: pH effects, isotherm modelling and implications for using TiO 2 for drinking water treatment, Chemosphere 174 (2017) 363–370.
[157] R. Rezaei, M. Mohseni, Impact of natural organic matter on the degradation of 2, 4-dichlorophenoxy acetic acid in a fluidized bed photocatalytic reactor, Chem. Eng. J. 310 (2017) 457–463.
[158] M. Long, J. Brame, F. Qin, J. Bao, Q. Li, P.J. Alvarez, Phosphate changes effect of humic acids on TiO2 photocatalysis: from inhibition to mitigation of electron–hole recombination, Environ. Sci. Technol. 51 (2016) 514–521.
[159] M.E. Pena, G.P. Korfiatis, M. Patel, L. Lippincott, X. Meng, Adsorption of As(V) and As(III) by nanocrystalline titanium dioxide, Water Res. 39 (2005) 2327–2337.
[160] Y. Wang, J. Duan, W. Li, S. Beecham, D. Mulcahy, Aqueous arsenite removal by simultaneous ultraviolet photocatalytic oxidation-coagulation of titanium sulfate, J. Hazard. Mater. 303 (2016) 162–170.
[161] S.-H. Yoon, J.H. Lee, Oxidation mechanism of As(III) in the UV/TiO2 system:-evidence for a direct hole oxidation mechanism, Environ. Sci. Technol. 39 (2005) 9695–9701.
[162] L. Ma, S.X. Tu, Removal of arsenic from aqueous solution by two types of nano TiO2 crystals, Environ. Chem. Lett. 9 (2011) 465–472.
[163] L. Xie, P. Liu, Z. Zheng, S. Weng, J. Huang, Morphology engineering of V 2 O 5/ TiO 2 nanocomposites with enhanced visible light-driven photofunctions for arsenic removal, Appl. Catal. B: Environ. 184 (2016) 347–354.
[164] Y. Kim, H. Joo, N. Her, Y. Yoon, J. Sohn, S. Kim, J. Yoon, Simultaneously photocatalytic treatment of hexavalent chromium (Cr(VI)) and endocrine disrupting compounds (EDCs) using rotating reactor under solar irradiation, J. Hazard. Mater. 288 (2015) 124–133.
[165] A. Laganà, A. Bacaloni, I. De Leva, A. Faberi, G. Fago, A. Marino, Analytical methodologies for determining the occurrence of endocrine disrupting chemicals in sewage treatment plants and natural waters, Anal. Chim. Acta 501 (2004) 79–88.
[166] K. Sornalingam, A. McDonagh, J.L. Zhou, Photodegradation of estrogenic endocrine disrupting steroidal hormones in aqueous systems: progress and future challenges, Sci. Total Environ. 550 (2016) 209–224.
[167] A. Mirzaei, Z. Chen, F. Haghighat, L. Yerushalmi, Removal of pharmaceuticals and endocrine disrupting compounds from water by zinc oxide-based photocatalytic degradation: a review, Sustain. Cities Soc. 27 (2016) 407–418.
[168] C.-H. Hung, C. Yuan, H.-W. Li, Photodegradation of diethyl phthalate with PANi/CNT/TiO 2 immobilized on glass plate irradiated with visible light and simulated sunlight—effect of synthesized method and pH, J. Hazard. Mater. 322 (2017) 243–253.
[169] R.-a. Doong, C.-Y. Liao, Enhanced photocatalytic activity of Cu-deposited N-TiO 2/ titanate nanotubes under UV and visible light irradiations, Sep. Purif. Technol. 179 (2017) 403–411.
[170] K. Davididou, E. Hale, N. Lane, E. Chatzisymeon, A. Pichavant, J.-F. Hochepied, Photocatalytic treatment of saccharin and bisphenol-A in the presence of TiO 2 nanocomposites tuned by Sn (IV), Catal. Today 287 (2017) 3–9.
[171] S. Kim, H. Cho, H. Joo, N. Her, J. Han, K. Yi, J.-O. Kim, J. Yoon, Evaluation of performance with small and scale-up rotating and flat reactors; photocatalytic degradation of bisphenol A, 17β–estradiol, and 17α–ethynyl estradiol under solar irradiation, J. Hazard. Mater. 336 (2017) 21–32.
[172] A. Tian, Y. Wu, K. Mao, Z. You, Z. Tan, J. Ke, Enhanced Performance of Surface Modified TiO2 Nanotubes for the Decomposition of Perfluorooctanoic Acid, AIP Conference Proceedings, AIP Publishing, 2017 pp. 020029.
[173] V.M. Mboula, V. Héquet, Y. Andrès, Y. Gru, R. Colin, J. Doña-Rodríguez, L. Pastrana-Martínez, A. Silva, M. Leleu, A. Tindall, Photocatalytic degradation of estradiol under simulated solar light and assessment of estrogenic activity, Appl. Catal. B: Environ. 162 (2015) 437–444.
[174] G. Doná, J.L.A. Dagostin, T.A. Takashina, F.d. Castilhos, L. Igarashi-Mafra, A comparative approach of methylparaben photocatalytic degradation assisted by UV-C UV-A and vis radiations, Environ. Technol. (2017) 1–43.
[175] R. López Fernández, H.M. Coleman, P. Le-Clech, Impact of operating conditions on the removal of endocrine disrupting chemicals by membrane photocatalytic reactor, Environ. Technol. 35 (2014) 2068–2074.
[176] H.G. Oliveira, L.H. Ferreira, R. Bertazzoli, C. Longo, Remediation of 17-α-ethinylestradiol aqueous solution by photocatalysis and electrochemically-assisted photocatalysis using TiO 2 and TiO 2/WO 3 electrodes irradiated by a solar simulator, Water Res. 72 (2015) 305–314.
[177] A. Hernández-Gordillo, S. Obregón, F. Paraguay-Delgado, V. Rodríguez-González, Effective photoreduction of a nitroaromatic environmental endocrine disruptor by AgNPs functionalized on nanocrystalline TiO 2, RSC Adv. 5 (2015) 15194–15197.
[178] V. Kalarivalappil, C. Divya, W. Wunderlich, S.C. Pillai, S.J. Hinder, M. Nageri, V. Kumar, B.K. Vijayan, Pd loaded TiO2 nanotubes for the effective catalytic reduction of p-nitrophenol, Catal. Lett. 146 (2016) 474–482.
[179] M. Grung, Y. Lin, H. Zhang, A.O. Steen, J. Huang, G. Zhang, T. Larssen, Pesticide levels and environmental risk in aquatic environments in China—a review, Environ. Int. 81 (2015) 87–97.
[180] R.K. Ghosh, D.P. Ray, S. Chakraborty, K. Majumdar, D. Reddy, Pesticides in environment and their management strategies, Int. J. Bioresour. Sci. 2 (2015) 47.
[181] H. Hidaka, T. Kurihara, N. Serpone, Photo-assisted Mineralization of the Agrochemical Pesticides Oxamyl and Methomyl and the Herbicides Diphenamid and Asulam, Environmentally Benign Photocatalysts, Springer, 2010, pp. 321–344.
[182] D. Alrousan, M. Polo-López, P. Dunlop, P. Fernández-Ibáñez, J. Byrne, Solar photocatalytic disinfection of water with immobilised titanium dioxide in re-circulating flow CPC reactors, Appl. Catal. B: Environ. 128 (2012) 126–134.
[183] M. Jiménez, M. Ignacio Maldonado, E.M. Rodríguez, A. Hernández-Ramírez, E. Saggioro, I. Carra, J.A. Sánchez Pérez, Supported TiO 2 solar photocatalysis at semi-pilot scale: degradation of pesticides found in citrus processing industry wastewater, reactivity and influence of photogenerated species, J. Chem. Technol. Biotechnol. 90 (2015) 149–157.
[184] S.J. Jafari, G. Moussavi, H. Hossaini, Degradation and mineralization of diazinon pesticide in UVC and UVC/TiO 2 process, Desalin. Water Treat. 57 (2016) 3782–3790.
[185] M. Gar Alalm, A. Tawfik, S. Ookawara, Comparison of solar TiO 2 photocatalysis and solar photo-fenton for treatment of pesticides industry wastewater: operational conditions, kinetics, and costs, J. Water Process Eng. 8 (2015) 55–63.
[186] I. Salgado-Tránsito, A.E. Jiménez-González, M.L. Ramón-García, C.A. Pineda-Arellano, C.A. Estrada-Gasca, Design of a novel CPC collector for the photodegradation of carbaryl pesticides as a function of the solar concentration ratio, Sol. Energy 115 (2015) 537–551.
[187] S. Gomez, C.L. Marchena, M.S. Renzini, L. Pizzio, L. Pierella, In situ generated TiO2 over zeolitic supports as reusable photocatalysts for the degradation of dichlorvos, Appl. Catal. B: Environ. 162 (2015) 167–173.
[188] O. Sacco, V. Vaiano, C. Han, D. Sannino, D.D. Dionysiou, Photocatalytic removal of atrazine using N-doped TiO 2 supported on phosphors, Appl. Catal. B: Environ. 164 (2015) 462–474.
[189] C. Qin, S. Yang, C. Sun, M. Zhan, R. Wang, H. Cai, J. Zhou, Investigation of the effects of humic acid and H2O2 on the photocatalytic degradation of atrazine assisted by microwave, Front. Environ. Sci. Eng. China 4 (2010) 321–328.
[190] T. McMurray, P. Dunlop, J. Byrne, The photocatalytic degradation of atrazine on nanoparticulate TiO 2 films, J. Photochem. Photobiol. A: Chem. 182 (2006) 43–51.
[191] L. Zheng, F. Pi, Y. Wang, H. Xu, Y. Zhang, X. Sun, Photocatalytic degradation of acephate, omethoate, and methyl parathion by Fe 3 O 4@ SiO 2@ mTiO 2 nanomicrospheres, J. Hazard. Mater. 315 (2016) 11–22.
[192] S. Malato, P. Fernández-Ibáñez, M. Maldonado, J. Blanco, W. Gernjak, Decontamination and disinfection of water by solar photocatalysis: recent overview and trends, Catal. Today 147 (2009) 1–59.
[193] J. Podporska-Carroll, E. Panaitescu, B. Quilty, L. Wang, L. Menon, S.C. Pillai, Antimicrobial properties of highly efficient photocatalytic TiO 2 nanotubes, Appl. Catal. B: Environ. 176 (2015) 70–75.
[194] D.W. Synnott, M.K. Seery, S.J. Hinder, G. Michlits, S.C. Pillai, Anti-bacterial activity of indoor-light activated photocatalysts, Appl. Catal. B: Environ. 130 (2013) 106–111.
[195] J.A. Byrne, P.A. Fernandez-Ibanez, P.S. Dunlop, D. Alrousan, J.W. Hamilton, Photocatalytic enhancement for solar disinfection of water: a review, Int. J. Photoenergy 2011 (2011).
[196] C.W. Dunnill, Z. Ansari, A. Kafizas, S. Perni, D.J. Morgan, M. Wilson, I.P. Parkin, Visible light photocatalysts—N-doped TiO 2 by sol–gel, enhanced with surface bound silver nanoparticle islands, J. Mater. Chem. 21 (2011) 11854–11861.
[197] P. Wu, R. Xie, K. Imlay, J.K. Shang, Visible-light-induced bactericidal activity of titanium dioxide codoped with nitrogen and silver, Environ. Sci. Technol. 44 (2010) 6992–6997.
[198] A.A. Ashkarran, H. Hamidinezhad, H. Haddadi, M. Mahmoudi, Double-doped TiO 2 nanoparticles as an efficient visible-light-active photocatalyst and antibacterial agent under solar simulated light, Appl. Surf. Sci. 301 (2014) 338–345.
[199] J.C. Yu, W. Ho, J. Yu, H. Yip, P.K. Wong, J. Zhao, Efficient visible-light-induced photocatalytic disinfection on sulfur-doped nanocrystalline titania, Environ. Sci. Technol. 39 (2005) 1175–1179.
[200] J. Rengifo-Herrera, E. Mielczarski, J. Mielczarski, N. Castillo, J. Kiwi, C. Pulgarin, Escherichia coli inactivation by N, S co-doped commercial TiO 2 powders under UV and visible light, Appl. Catal. B: Environ. 84 (2008) 448–456.
[201] J. Rengifo-Herrera, K. Pierzchała, A. Sienkiewicz, L. Forro, J. Kiwi, C. Pulgarin, Abatement of organics and Escherichia coli by N, S co-doped TiO 2 under UV and visible light. Implications of the formation of singlet oxygen (1 O 2) under visible light, Appl. Catal. B: Environ. 88 (2009) 398–406.

[202] J. Rengifo-Herrera, J. Kiwi, C. Pulgarin, N, S co-doped and N-doped Degussa P-25 powders with visible light response prepared by mechanical mixing of thiourea and urea. Reactivity towards E. coli inactivation and phenol oxidation, J. Photochem. Photobiol. A: Chem. 205 (2009) 109–115.
[203] J.A. Rengifo-Herrera, C. Pulgarin, Photocatalytic activity of N, S co-doped and N-doped commercial anatase TiO 2 powders towards phenol oxidation and E. coli inactivation under simulated solar light irradiation, Sol. Energy 84 (2010) 37–43.
[204] M. Garvey, E. Panaitescu, L. Menon, C. Byrne, S. Dervin, S.J. Hinder, S.C. Pillai, Titania nanotube photocatalysts for effectively treating waterborne microbial pathogens, J. Catal. 344 (2016) 631–639.
[205] H. Chen, B. Wang, D. Gao, M. Guan, L. Zheng, H. Ouyang, Z. Chai, Y. Zhao, W. Feng, Broad-spectrum antibacterial activity of carbon nanotubes to human gut bacteria, Small 9 (2013) 2735–2746.
[206] M.B. Fisher, D.A. Keane, P. Fernandez-Ibanez, J. Colreavy, S.J. Hinder, K.G. McGuigan, S.C. Pillai, Nitrogen and copper doped solar light active TiO 2 photocatalysts for water decontamination, Appl. Catal. B: Environ. 130 (2013) 8–13.
[207] P. Radhika, Investigation into the growth phase dependent sensitivity of Mycobacterium aurum to chlorine and quantification of reactive oxygen species, Int. J. Sci. Technol. Res. 2 (7) (2013) 32–39.
[208] D.E. Helbling, J.M. VanBriesen, Free chlorine demand and cell survival of microbial suspensions, Water Res. 41 (2007) 4424–4434.
[209] C.-C. Wang, X.-D. Du, J. Li, X.-X. Guo, P. Wang, J. Zhang, Photocatalytic Cr (VI) reduction in metal-organic frameworks: a mini-review, Appl. Catal. B: Environ. 193 (2016) 198–216.
[210] Z. Wu, X. Yuan, J. Zhang, H. Wang, L. Jiang, G. Zeng, Photocatalytic decontamination of wastewater containing organic dyes by metal–organic frameworks and their derivatives, ChemCatChem 9 (2016) 41–64.
[211] C.-C. Wang, J.-R. Li, X.-L. Lv, Y.-Q. Zhang, G. Guo, Photocatalytic organic pollutants degradation in metal–organic frameworks, Energy Environ. Sci. 7 (2014) 2831–2867.
[212] E.M. Dias, C. Petit, Towards the use of metal–organic frameworks for water reuse: a review of the recent advances in the field of organic pollutants removal and degradation and the next steps in the field, J. Mater. Chem. A 3 (2015) 22484–22506.
[213] J. Zhao, D.T. Lee, R.W. Yaga, M.G. Hall, H.F. Barton, I.R. Woodward, C.J. Oldham, H.J. Walls, G.W. Peterson, G.N. Parsons, Ultra-fast degradation of chemical warfare agents using MOF–nanofiber kebabs, Angew. Chem. 128 (2016) 13418–13422.
[214] X. Li, Y. Pi, Q. Xia, Z. Li, J. Xiao, TiO 2 encapsulated in Salicylaldehyde-NH 2-MIL-101 (Cr) for enhanced visible light-driven photodegradation of MB, Appl. Catal. B: Environ. 191 (2016) 192–201.
[215] M.Y. Masoomi, M. Bagheri, A. Morsali, P.C. Junk, High photodegradation efficiency of phenol by mixed-metal–organic frameworks, Inorg. Chem. Front. 3 (2016) 944–951.
[216] L.-L. Liu, C.-X. Yu, J.-M. Du, S.-M. Liu, J.-S. Cao, L.-F. Ma, Construction of five Zn (II)/Cd (II) coordination polymers derived from a new linear carboxylate/pyridyl ligand: design, synthesis, and photocatalytic properties, Dalton Trans. 45 (2016) 12352–12361.
[217] S. Mosleh, M. Rahimi, M. Ghaedi, K. Dashtian, Sonophotocatalytic degradation of trypan blue and vesuvine dyes in the presence of blue light active photocatalyst of Ag 3 PO 4/Bi 2S 3-HKUST-1-MOF: central composite optimization and synergistic effect study, Ultrason. Sonochem. 32 (2016) 387–397.
[218] K. Liu, Y. Gao, J. Liu, Y. Wen, Y. Zhao, K. Zhang, G. Yu, Photoreactivity of metal–organic frameworks in aqueous solutions: metal dependence of reactive oxygen species production, Environ. Sci. Technol. 50 (2016) 3634–3640.

Ciara Byrne holds a B.Sc. (Hons) in Forensic Investigation and Analysis from the Institute of Technology Sligo, Ireland. During her undergraduate degree, Ciara completed a number of research projects regarding the identification of crystalline and amorphous phases using X-ray Diffraction (XRD) and Fourier Transfer Infrared (FTIR) spectroscopy, performed under the supervision of Professor Suresh Pillai. This research examined doped TiO_2 and how elevated temperatures effected the anatase-rutile transition. Ciara is currently studying for a PhD in the Anatase to Rutile Transition in Titanium Dioxide Nanomaterials, with Prof. Suresh Pillai as her supervisor. Ciara's research interests are mainly in the areas of material chemistry, titanium dioxide, sol-gel technology, photocatalysis and applications of photocatalysis.

Dr. Gokulakrishnan Subramanian is a postdoctoral researcher at Department of Chemical Engineering, Indian Institute of Science in the group of Professor Giridhar Madras. He is studying photocatalysis based Advanced Oxidation Processes for decontamination of waste water. He received his Ph.D. degree in Chemistry from BITS-Pilani K.K Birla Goa Campus in 2015 under the mentorship of Professor Halan Prakash, where he studied the activation of peroxo compounds for oxidative degradation of organic and microbial pollutants. He received his Master's degree in Molecular biosciences from Bharathidasan University, and BSc (Hons) in Biosciences from Sathya Sai Institute of Higher Learning.

Prof. Suresh C. Pillai has obtained his PhD in the area of Nanotechnology from Trinity College (TCD), The University of Dublin, Ireland and then performed a postdoctoral research at California Institute of Technology (Caltech), USA. He has then worked at CREST in DIT as a senior scientist responsible for nanotechnology research before moving to Institute of Technology Sligo as a senior lecturer in environmental nanotechnology. He is an elected fellow of the Royal Microscopical Society (FRMS) and the Institute of Materials, Minerals and Mining (FIMMM). He is responsible for acquiring more than €3 million direct R & D funding. Prof. Pillai is a recipient of a number of awards for research accomplishments including the 'Industrial Technologies Award 2011′ from Enterprise Ireland for commercialising nanomaterials for industrial applications. He was also the recipient of the 'Hothouse Commercialisation Award 2009′ from the Minister of Science, Technology and Innovation and also the recipient of the 'Enterprise Ireland Research Commercialization Award 2009′. He has also been nominated for the 'One to Watch' award 2009 for commercialising R & D work (Enterprise Ireland). One of the nanomaterials based environmental technologies developed by his research team was selected to demonstrate as one of the fifty 'innovative technologies' (selected after screening over 450 nominations from EU) at the first Innovation Convention organised by the European Commission on 5–6th December 2011. He is the national delegate and technical expert for ISO standardization committee and European standardization (CEN) committee on photocatalytic materials.